Review Article

Laminar Flame Characteristics of 2,5-Dimethylfuran (DMF) Biofuel: A Comparative Review with Ethanol and Gasoline

Long Vuong Hoang[1], Danh Chan Nguyen[2,*], Thanh Hai Truong[3], Huu Cuong Le[3], Minh Nhat Nguyen[4,*]

[1]*Faculty of Mechanical Engineering, Industrial University of Ho Chi Minh City (IUH), Ho Chi Minh City, Vietnam*

[2]*Institute of Mechanical Engineering, Ho Chi Minh City University of Transport, Ho Chi Minh City, Vietnam*

[3]*Institute of Maritime, Ho Chi Minh City University of Transport, Ho Chi Minh City, Vietnam*

[4]*Institute of Engineering, HUTECH University, Ho Chi Minh City, Vietnam*

Abstract. Since the early years of the 21st century, the whole world has faced two very urgent problems: the depletion of fossil energy sources and climate change due to environmental pollution. Among the solutions sought, 2,5-Dimethylfuran (DMF) emerged as a promising solution. DMF is a 2nd generation biofuel capable of mass production from biomass. There have been many studies confirming that DMF is a potential alternative fuel for traditional fuels (gasoline and diesel) in internal combustion engines, contributing to solving the problem of energy security and environmental pollution. However, in order to apply DMF in practice, more comprehensive studies are needed. Not out of the above trend, this paper analyzes and discusses in detail the characteristics of DMF's combustible laminar flame and its instability under different initial conditions. The evaluation results show that the flame characteristics of DMF are similar to those of gasoline, although the burning rate of DMF is much higher than that of gasoline. This shows that DMF can become a potential alternative fuel in internal combustion engines.

1. Introduction

The world is facing very serious problems stemming from the excessive use of natural resources along with the increase in activities that pollute the atmosphere. The excessive global increase in greenhouse gas (Ölçer *et al.*, 2021), particulate materials (Nayak *et al.*, 2020), and nitrogen oxide emissions (Le *et al.*, 2021)(Chau *et al.* 2020) is changing the global climate(Geo *et al.*, 2021). In the context of the Covid-19 pandemic that is spreading around the world and threatening all the achievements of any economy, policies on sustainable energy and effective emission control have become all the more urgent (Pradhan *et al.*, 2020)(Klemeš *et al.*, 2021)(Huynh *et al.*, 2021)(Hadiyanto *et al.*, 2021). In the last decade, biofuels have emerged as a useful solution to two problems facing countries around the world: the depletion of fossil fuel resources and environmental pollution (Tabatabaei *et al.*, 2020)(Arias-Fernández *et al.*, 2020)(Wahyono *et al.*, 2020). Therefore, research on biofuels has been widely carried out on a global scale, especially on biofuels of the 2nd and 3rd generations (Kumar and Bharadvaja, 2020)(Xuan and Viet, 2021)(Nikkhah *et al.*, 2019)(Christwardana *et al.*, 2020). Among them, biofuels derived from cellulosic biomass are considered a potential candidate due to their feasibility (Abyaz *et al.*, 2020)(Bamisile *et al.*, 2020)(Wang and Yao, 2020). Among these, ethanol (a kind of biofuel extracted from biomass) has been used by many countries as an alternative to traditional gasoline fuel because ethanol can be produced in large quantities (Ramamoorthy *et al.*, 2020)(Ma'As *et al.*, 2020)(Praveena *et al.*, 2021). However, due to its inherent disadvantages (low energy density, water-solubility, etc.), increasing the mixing ratio of ethanol to gasoline also faces many obstacles. Recently, the production of 2,5 dimethylfuran (DMF) from biomass has made great progress, showing that DMF has potential for industrial-scale production from an inexhaustible source of biomass (Wang *et al.*, 2019). Therefore, DMF has emerged as an alternative fuel for traditional fuels such as gasoline and diesel in internal combustion engines because it has many similar properties to gasoline (Chau *et al.*, 2020)(Aykut and Sandro, 2021) (as shown in Table 1).

---

* Corresponding author: Danh Chan Nguyen (chan.nguyen@ut.edu.vn); Minh Nhat Nguyen (nm.nhat@hutech.edu.vn)

Table 1

Comparison of physicochemical properties between gasoline, ethanol, and DMF (An *et al.*, 2013)(Chan, 2018)(Dutta, 2012)(Hu *et al.*, 2020)

Properties	Gasoline	Ethanol	DMF
Chemical formula	C_4–C_{12}	C_2H_6	C_6H_8O
ρ	749	795	893
LHV	347	910	393
A/F	14.75	8.90	10.6
O.C	0	34.78	16.67
μ	0.35-0.45	1.52	0.6
σ	0.0207	0.0213	0.0236
BP	27-220	74	96
Energy density	32-35	17.9-21.4	29.4
AIT	410	430	276
RON	90-100	110	119

ρ: Density of the liquid (kg/m³); LHV: Latent heat of vaporization (kJ/kg); A/F: Stoichiometric air/fuel ratio; O.C: Oxygen content (%); μ: Kinematic viscosity (cSt); σ: Surface tension (N/m); BP: Boiling point (ºC); AIT: Auto-ignition temperature (ºC); RON: Research octane number

From Table 1, it can be easily seen that compared with ethanol, DMF has many advantages such as higher energy density and octane number (Daniel *et al.*, 2012a)(Daniel *et al.*, 2012b). Especially, unlike ethanol, DMF is almost insoluble in water, so it is easier to mix them with commercial gasoline. Many studies have confirmed that it is possible to use DMF as fuel on internal combustion engines (including SI and CI engines) without changing the engine structure (Liu *et al.*, 2019) (Wei *et al.*, 2017)(Alami *et al.*, 2021). In addition, the use of DMF as a fuel also helps to reduce harmful emissions more than the use of traditional fuels (Zhang *et al.*, 2013)(Chen *et al.*, 2013). Besides, through the study and comparison of flame propagation and laminar burning velocity (LBV), researchers have shown that DMF has quite similar combustion properties to gasoline (Lifshitz *et al.*, 1998)(Peña *et al.*, 2018)(Djokic *et al.*, 2013)(Tuan Anh, 2020). The propagation characteristic of the laminar flame is a very important characteristic to help better understand the combustion and emission formation when using DMF as engine fuel (Badawy *et al.*, 2016)(Chu *et al.*, 2020). Therefore, the study of the laminar flame characteristics of DMF is very important and necessary. This paper presents a study on the laminar flame characteristics of DMF as well as the factors affecting

these characteristics through a comparison of the burning process of DMF with gasoline and ethanol.

2. DMF synthesis pathway

Currently, the conversion of cellulose biomass to DMF is accomplished through two steps (Figure 1): The first step is to pre-treat the biomass and reduce it to glucose or fructose, then dehydration to generate to 5-hydroxymethylfurfural (HMF); The next step is to convert HMF to DMF through hydrodeoxygenation (HDO) (Ong and Wu, 2020)(Ong *et al.*, 2021b)(Katagi *et al.*, 2021).

Biomass pretreatment is an essential process to improve the efficiency of lignocellulose conversion into value-added energy products (Zullaikha *et al.*, 2021). Recent literature has presented many efficient biomass pretreatment techniques based on the background of biological, chemical, and physical treatment methods (Ab Rasid *et al.*, 2021). The pretreatment of biomass with liquid acid has been claimed to be the most popular because of its high conversion efficiency in a shorter time (Cheng *et al.*, 2021)(Xuan *et al.*, 2021)(Chong *et al.*, 2021). Furthermore, this technique has contributed significantly to the reduction of unwanted by-products in the biorefinery. However, the negative impacts of liquid waste from chemical pretreatment processes on the environment have been major challenges. Liquid hot water pretreatment is becoming a potential and environmentally friendly biomass treatment technique as well as with excellent hemicellulose removal and reduction of simple sugars (Weerasinghe *et al.*, 2021)(J. Zhang *et al.*, 2020)(Chen *et al.*, 2021). The disadvantage of biomass pretreatment with liquid hot water is that the dilution effect of the liquid stream reduces the efficiency of the subsequent fermentation in the biofuel conversion pathway (Kadarwati *et al.*, 2021)(Vieira *et al.*, 2020). Recently, microwave irradiation, a method that combines physics and chemistry, has attracted a lot of attention from researchers about biorefineries from biomass due to economic and environmental benefits (Ong *et al.*, 2021a)(Ong and Wu, 2020)(Lin *et al.*, 2021). Overall, the development of biomass pretreatment technology has contributed greatly to the driving force behind the production of bioenergy and valuable products such as furan-based fuels (HMF, MF, and DMF) (Viet Pham and Tuan Hoang, 2021)(Xu *et al.*, 2016)(Cheng *et al.*, 2021).
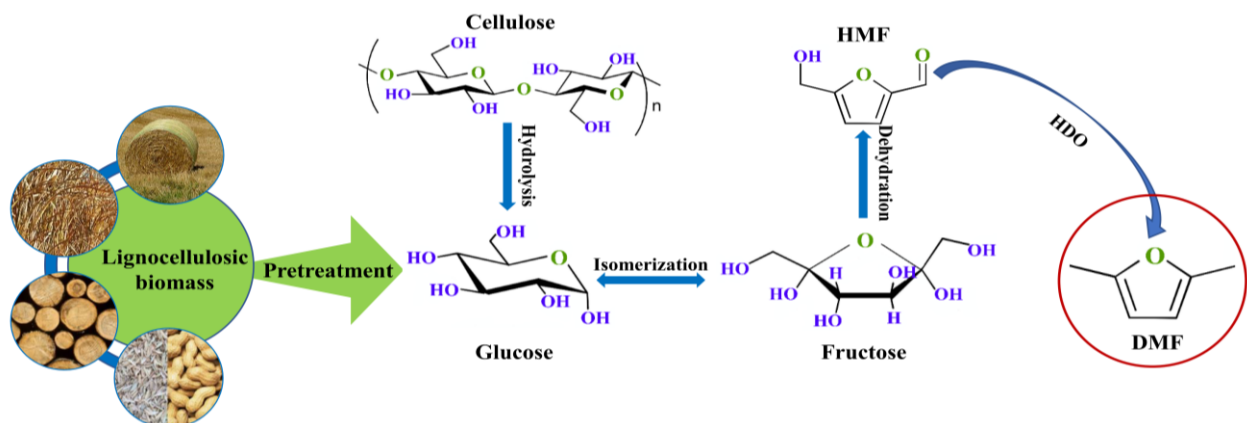
Fig 1. DMF production pathway (Aykut and Sandro, 2021)

Many studies have shown that the yield of DMF obtained in the production process from biomass varies greatly depending on the reaction conditions, the type of catalyst, and the solvent used, even as a hydrogen donor (Bohre *et al.*, 2015). Y. Román-Leshkov et al. (Román-Leshkov *et al.*, 2007) proposed a two-step DMF production process: the first step is dehydration to convert fructose into HMF with HCl catalysis; the next step is to carry out the HDO process to convert HMF to DMF with Cu/Ru catalyst. The authors reported that the production process achieved an efficiency of up to 71% at the reaction temperature of 220°C and 6.8 bar of H_2 pressure. Similarly, Binder et al. (Binder and Raines, 2009) also used Cu/Ru catalyst in the HDO process to convert HMF to DMF with the yield of this process being 49%. M. Chidambaram et al. (Chidambaram and Bell, 2010) experimented using EMIMCl/acetonitrile solvent with the catalyst as Pd/C under the temperature condition of 120 °C and the reaction time was 1 hour. This conversion is also 49% efficient, similar to what Binder et al. have done before. Under similar reaction conditions (temperature at 130°C, H_2 pressure at 7 bar) but Lu et al. (Zu *et al.*, 2014) used a catalyst as Ru/Co_3O_4 and obtained an unexpectedly high efficiency, up to 93%. In another work, Chen et al. (Chen *et al.*, 2020) reported that the efficiency of the HDO reaction to convert HMF to DMF was up to 94% using Fe-Co-Ni/h-BN as a catalyst. More specifically, this catalyst can be reused ten times and still achieve complete HMF conversion efficiency, while the conversion efficiency to DMF is slightly reduced but still above 82%. In a different direction of research, Nishimura et al. (Nishimura *et al.*, 2014) developed a bimetallic catalytic system Pd50Au50/C in the presence of HCl acid and the results obtained were very impressive: the reaction efficiency was up to 96% after 6 hours at the reaction temperature 60°C. Following this success, more and more attention has been paid to the development of bimetallic catalyst systems and all achieved very high reaction yields: Cu/Ni (91.1%) (Zhang *et al.*, 2019), Cu-Ni/BC (93.5%) (Zhu *et al.*, 2019), 10Cu-1Pd/RGO (95%) (Mhadmhan *et al.*, 2019), Ni-MoS2/mAl2O3 (95%) (Han *et al.*, 2020), Ni-Fe/TiO2 (97%) (Przydacz *et al.*, 2020)(Syukri *et al.*, 2021).

Besides the studies on the effect of the catalyst, many studies also mention the effect of hydrogen addition for the HDO process when converting HMF to DMF. Formic acid is considered a common source of hydrogen addition in the preparation of DMF from biomass, but the yield is not high, only about 32% (Dutta *et al.*, 2012). To improve this, Hu et al. (B. Hu et al., 2020) showed that the multifunctional Pd is supported on the N-doped neutral carbon-catalyzed HDO of HMF using formic acid as the hydrogen source, generating 97% of the DMF.

In this work, Mhadmhan et al. (Mhadmhan *et al.*, 2019) reported that efficiency was achieved up to 95% using 2-propanol as the hydrogen addition source for HDO of HMF, using Cu-Pd bimetallic catalysts incorporated on graphene oxide. In another study, Feng et al. (Feng *et al.*, 2020) investigated the effect of ethanol as a hydrogen donor on DMF yield using Ru/ZSM-5 as the catalyst, the results obtained were unexpected, up to 97%. In all the methods mentioned above, the important step is the hydrolysis of C-O to C-H in the presence of a catalyst. Indeed, the precious metals were found to be more selective than the non-precious metals.

3. Laminar flame characteristics

The laminar burning velocity (LBV) is a very important property of the fuel. It is very important in the study of engine combustion and is especially important in the simulation of combustion (Teraji *et al.*, 2005). For models to study the phenomenon of combustion, it is extremely necessary to fully determine the kinetic-chemical factors and the reaction of the flame (Fenton, 1998)(Noor *et al.*, 2018). However, due to the complexity and unstable nature of the turbulent motion inside the combustion chamber, most numerical simulation models rely on the laminar burning velocity to describe and explain the turbulent components instead (Ohyagi *et al.*, 2010). Indeed, the laminar burning velocity directly affects the combustion rate and thereby affects the efficiency of the engine (Benson and Whitehouse, 2013)(Nayak *et al.*, 2017). Normally, a fuel's high combustion rate can bring many benefits and improve engine performance, but it can also lead to excessively high combustion pressure and temperature. On the contrary, the low combustion rate of the fuel could harm its economic characteristics (Tian *et al.*, 2010)(İlçin and Altun, 2021). The laminar burning velocities can be studied from a stationary homogeneous mixture, such as in a constant volume vessel. It is possible to describe the laminar burning velocity as a function of temperature and combustion pressure, and these equations have also been mentioned in many studies (Huang *et al.*, 2006)(Bradley *et al.*, 2007)(Burke *et al.*, 2009)(Chen *et al.*, 2009)(Wu *et al.*, 2011). From these equations, it can be seen that the laminar burning velocity is a strong function of initial temperature and a weak function of pressure. Thus, to provide a deeper understanding of the combustion process of the fuel in the engine, many works have focused on studying the characteristics of the flame as a basis for further research on the release of energy as well as the formation of pollutants inside the engine. Therefore, LBV is considered an important parameter in flame characterization study, and the method of LBV study can be given in Table 2.

In order to be used as a fuel in an internal combustion engine, the combustion characteristics of DMF need to be studied carefully and in detail because it is a new chemical. Many parameters characterize the combustion of fuel, but among them, two parameters are considered to represent the combustion characteristics and are the basis for determining the chemical reaction mechanisms that take place while burning: laminar burning velocity (LBV) and unstretched flame propagation speed (UFPS) (Law, 2010). Due to the combined influence of many stakeholders such as the physicochemical properties of the fuel, the reaction mechanism of the compound components taking place during combustion, it is easy to see that the initial parameters of the combustion process such as pressure, temperature, equivalence ratio, the composition of the mixture significantly affect LBV (Xu *et al.*, 2016)(Pham, 2019). LBV is the combustion rate of fuel in an internal combustion engine and is considered a very important indicator to simulate the turbulent processes taking place inside the engine during combustion. The heat flux-based method or the use of combustion bombs under isochoric conditions were concentrated by investigators.

Table 2
The studies of laminar burning velocities (LBV) of DMF combustion and kinetic in different conditions

| Method	T (K)	P (bar)	Others	Ref.
Constant volume bomb	393	1	dilutions: 0–15% (N_2 and CO_2); equivalent ratios 0.9÷1.5;	(Wu *et al.*, 2009)
	373; 348; 323	1	equivalent ratios 0.6÷2.0;	(Tian *et al.*, 2010)
	393	7.5; 5; 2.5; 1	equivalent ratios 0.8÷1.5;	(Wu *et al.*, 2010)
	393	1	dilutions: N_2 and CO_2; equivalent ratios 0.9÷1.5;	(Li *et al.*, 2012)
Heat flux combustor	473; 433; 393	5; 2.5; 1	equivalent ratios 0.9÷1.5;	(Wu *et al.*, 2012)
	473; 393; 298	1	equivalent ratios 1.1÷1.2;	(Bhattacharya and Datta, 2019)
Flat-flame combustor	358; 298	1	equivalent ratios 0.9÷1.5;	(Somers *et al.*, 2013)

Because DMF is considered a fuel of internal combustion engines, during the study of its combustion characteristics, it was found that there is a close correlation between UFPS and the stability of the flame during the ignition process of this fuel. In general, previous studies on the combustion characteristics of DMF were conducted in two directions: the study of the combustion characteristics of pure DMF or the study of the combustion characteristics of the mixtures of DMF-petrol, DMF-diesel corresponding with different mixing ratios(Le and Hoang, 2017). In addition to the above problems, studies on the combustion characteristics of DMF also refer to the Markstein length of this fuel. This is a very important parameter of combustion because the Markstein length has a significant influence on the stability of the flame. In particular, it is a fact that the thermal diffusion effects of the flame must be accepted in the appropriate region, so the Markstein length below zero represents the instability of the flame. This parameter will be further mentioned in the next section.

3.1. Laminar burning velocity

Wu et al. (Wu *et al.*, 2009) conducted the earliest study of LBV by DMF. The experiments were conducted to measure the LBV parameters and Markstein length of the DMF-air-N_2/CO_2 premixed mixture, corresponding to a reaction temperature of 393K and pressure of 1 atm. During the measurement, the equivalence ratio is modified by 0.9 ÷1.5, and the dilution ratio ranges 0÷15%. The image of the flame when burning is measured and recorded with the help of high-speed schlieren imaging equipment. Research results showed that as the dilution percentage increases, the LBV of the mixture will decrease, leading to an increase in flame stability. At the same time, Markstein's length also increased with increasing dilution ratio. When using different diluents CO_2 and N_2, the study results showed that CO_2 diluent has a greater impact on Markstein length, LBV, and flame stability than using N_2 as the diluent. In addition, the research results also showed that the flame of the fuel-lean mixture is more stable than that of the fuel-rich mixture. Besides, Figure 2 also depicts the relationship between LBV and dilution ratio. In this figure, the effect of diluents including N_2 and CO_2 can be easily observed on the premix flame of the DMF. In addition, the authors also concluded that the maximum LBV was in the 1.1÷1.2 range of the equivalence ratio and it did not change, even with the addition of diluent (Wu *et al.*, 2009). Li and co-workers (Li *et al.*, 2012) conducted another study to

determine the laminar flame characteristics of the DMF/iso-octane mixture. Experiments were conducted at initial conditions of 393K temperature and 1bar pressure, using (15% N_2 + 85% CO_2) as diluent/air. Research results show that the stability of the flame decreases slightly with the increasing sing concentration of DMF in the mixture, while LBV has almost no fluctuation. At the same time, the study results also confirm that at unchanged equivalence ratio, the flame stability is improved with increasing dilution ratio.

To evaluate the effect of pressure on the LBV of a spherical flame that expands when using a DMF-air mixture, Wu et al. (Wu *et al.*, 2011) conducted experiments at a fixed temperature of 393 K, with a pressure variation from 1÷7.5 bar. Experimental results show that flame instability increases with higher pressure according to a bigger equivalence ratio. In another study, Wu et al. (Wu *et al.*, 2010) conducted the experiment with a constant initial pressure of 1 atm but the initial temperature of the experiment changed correspondingly with different levels (393 K, 433 K, and 473 K), in order to measure and evaluation of the LBV and UFSP of the DMF/air mixture. The research results show that LBV and UFPS reached the peak value corresponding to an equivalence ratio of 1.2. Besides, when increasing the initial temperature of the reaction, the Markstein length has a marked increase. Conversely, when increasing the equivalent ratio, the Markstein length decreases.
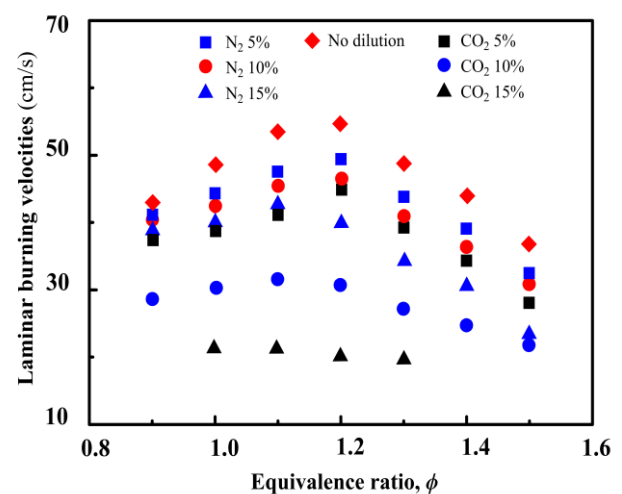
Fig 2. Relation between LBV and Φ in the initial pressure at the fixed temperature of 393K (Wu *et al.*, 2009)(Wu *et al.*, 2010)(Tian *et al.*, 2019)(Ma *et al.*, 2013)

In growth of reaction temperature at the beginning phase, the peak value of UFPS tends to move to the DMF-rich mixture region, while the peak of LBV has almost no change. Importantly, the LBV of the DMF/air mixture was investigated to provide important background data for sequential studies. To determine the burning velocity of fuel, it is very important to determine the LBV for different fuels, especially compared to traditional fuels (Wirawan *et al.*, 2014). In order to have clearer and more convincing evidence of the applicability of DMF as an alternative fuel in gasoline engines, DMF's LBV needs to be compared with commercially available fuels such as iso-octane, gasoline, and bioethanol (Li *et al.*, 2021)(Vinh *et al.*, 2018). In this direction, the distinction between the LBV of DMF and iso-octane was investigated by Ma and co-workers (Ma *et al.*, 2014a) at constant pressure but under different initial temperatures. Similarly, LBVs of DMF, gasoline, and bioethanol were studied and compared by Tian *et al.* (Tian *et al.*, 2010) under the change of equivalent ratio. The influence of initial pressure and temperature, fuel types, and diluents on the parameters of LBV, UFPS, and Markstein length can be easily seen from the studies mentioned above and can be represented corresponding to the ignition mixture in the engine combustion chamber. These works can be considered as core studies and are the foundation for the following studies on the application of DMF to engines. Figure 3 depicts the relationship between the equivalence ratio and the LBV when changing the initial parameters. Here, there is a consensus of studies on the trend of changes in LBV under different survey conditions. Specifically, the LBV results of the DMF/air mixture at the early stage temperature of 393K corresponds to the different pressures suggested by Wu et al (Wu *et al.*, 2009)(Wu *et al.*, 2010), Ma et al (Ma *et al.*, 2013), and Tian et al (Tian *et al.*, 2019) have been depicted in Figure 2. However, the data obtained from Ma et al. (Ma *et al.*, 2013) and Wu et al. (Wu *et al.*, 2009)(Wu *et al.*, 2010) are quite different, indicating that great uncertainty exists in the experimental results.
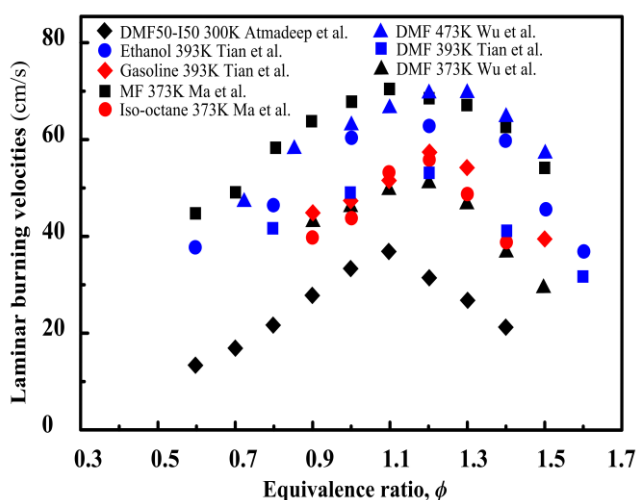
To study the effect of initial pressure on LBV, Galmiche et al. (Galmiche *et al.*, 2012) conducted experiments with two fuels, DMF and D20-I80 (20%vol. DMF + 80%vol. iso-octane). Experiment results show that the growth of the initial pressure, LBV decreases for both test fuels. The main reason is the rise of the initial pressure, the free current density, and also the laminar flux, leading to a decrease in LBV and Markstein length. In addition, radical termination reactions were found to be highly pressure-dependent (Galmiche *et al.*, 2012). Research results also show that the LBV of the D20-I80 mixture is lower than that of pure DMF under the same measurement conditions.

Studies on the effect of initial temperature on DMF's LBV have shown that in the same experimental configuration, the LBV of the test fuel will increase with increasing initial temperature. These results when conducted with DMF as fuel are similar to those obtained when other testing fuels (Han *et al.*, 2019)(Konnov *et al.*, 2018). Typically, improvement of the reduction mechanism for DMF has been confirmed based on LBV at different initial pressures and temperatures. To do this, Somers et al. (Somers *et al.*, 2013) used the heat flux method to measure the LBV of the DMF/air mixture at 298K, 358K, and 1atm with equivalent ratios of 0.6÷1.6. Tian et al. (Tian *et al.*, 2019) used the data obtained from this work to conduct their studies. In addition, also to determine the LBV of the DMF/air mixture, Ma et al. (Ma *et al.*, 2013) conducted tests at a temperature of 393 K and pressure of 1 atm. From Figure 2, according to the results from the numerical simulation of Tian et al. (Tian *et al.*, 2019), it is easy to see that the simulation results for the reduction mechanism in this survey improved by about 6% compared to those who performed the study under the same conditions (Minh and Anh, 2018)(Al-Tawaha *et al.*, 2018). This shows that the simulation and experimental results have very high similarities. At the same time, this result also indicates that a small impact of the LBV reduction mechanism has not been investigated in previous studies. Besides, the above works have also shown that LBV reaches its maximum value at a position close to the equivalent ratio (Φ) of 1.1. As a result of product dissociation and reduced exothermic, laminar flame peaks are found in fuel-rich regions. And most importantly, the graph in Figure 3 compiled from studies shows the great similarity between simulation and experimental results. Besides the temperature, pressure and equivalence ratio, the reactions between hydrocarbons and hydrogen atoms also affect LBV. To implement combustion control strategies in low-temperature engines, the intake air needs to be diluted (Van Pham and Anh Hoang, 2020). Therefore, one of the leading strategies commonly used is exhaust gas recirculation (Cao *et al.*, 2020). The gas components added during dilution also match the actual operating conditions of the engine. Therefore, in order to make better predictions about the performance of engines using DMF, the investigation of the dilution effects of N_2 and CO_2, as well as the mixing ratio on LBV, should also be taken into account (Xu *et al.*, 2016).

Figure 3 depicts a comparison of the LBV of DMF with other fuels. On this figure, it is easy to see that when the equivalence ratio is between 1.1 and 1.2, the LBV of the DMF reaches its maximum value. In general, when the

Fig 3. Effects of fuel types at the various temperatures on the relation between LBV and Φ (Tian *et al.,* 2010)(Wu *et al.,* 2010)(Bhattacharya and Datta, 2019)(Ma *et al.,* 2014a)

equivalence ratio is lower than 1.1, the LBV changes with a relatively stable pattern. But for equivalence ratios higher than 1.1, the change in LBV follows a disturbance trend (Tian *et al.*, 2010)(Wu *et al.*, 2010)(Bhattacharya and Datta, 2019)(Ma *et al.*, 2014a). The cause of this disturbance change may be because the experiments were conducted at different temperatures. At 373K, studies show that the LBV of iso-octane and DMF are lower than MF at all values of the equivalence ratio. The LBV of iso-octane and DMF reaches its maximum value at the equivalence ratio of 1.2, while the LBV of MF reaches the peaks at the equivalence ratio of 1.1. In their study, Ma et al. (Ma *et al.*, 2013) also reported similar results. Also in this work, the authors have shown that the UFPS of MF is faster by 30% and 50% compared to DMF and iso-octane, and the burning rate of MF is considered to be the highest of all tests conditions. Figure 4 depicts the schlieren

images of the DMF-based mixtures under different conditions. Where, Figure 4a presents a schlieren image of the corresponding DMF/air mixture with equivalence ratios of 1.2 and different dilution ratios (Li *et al.*, 2012). With the increasing dilution ratio, some cracks can be seen on the smooth flame surfaces. However, these cracks have no significant effect on the manner of the flame velocity propagates because of their unbranching(Tse *et al.*, 2000)(Nayak and Mishra, 2016). Especially under this condition, the correlation between the expansion rate and the elongation rate of the flame propagation is linear. It is worth mentioning that the area in front of the flame can increase with the appearance of an unstable flame, leading to a reaction on the flame surface and its self-acceleration or self-turbulence (Williams, 2018).
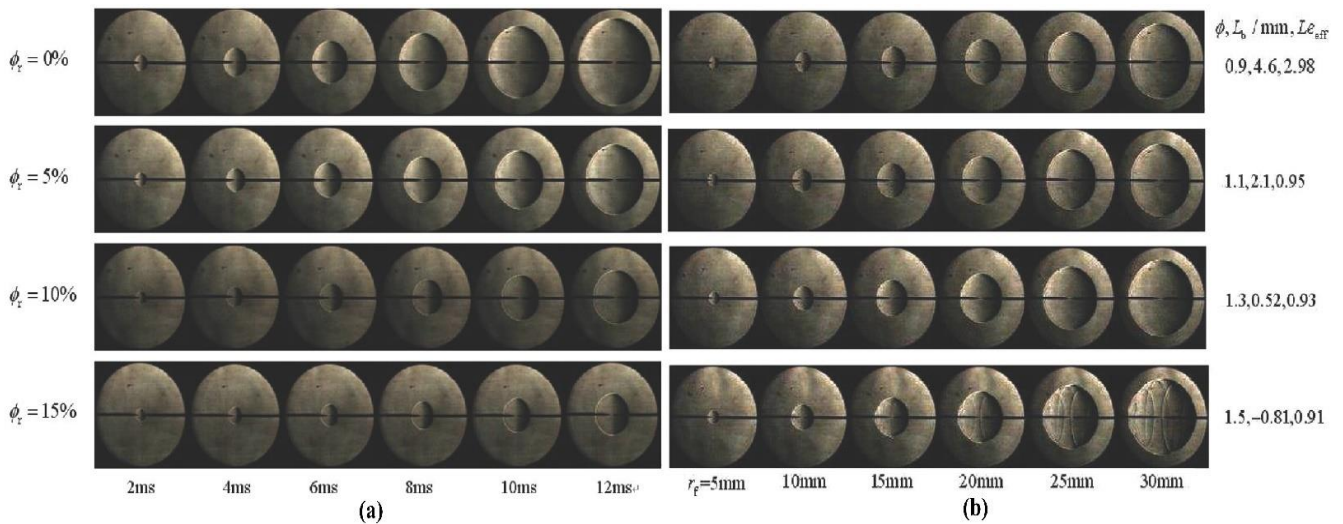

Fig 4. DMF mixture flame Schlieren images in different conditions; (a) - At the 1.2 equivalent ratio and different dilution ratios; (b) – For DMF/iso-octane (20/80), at four equivalent ratios (Li *et al.*, 2012)
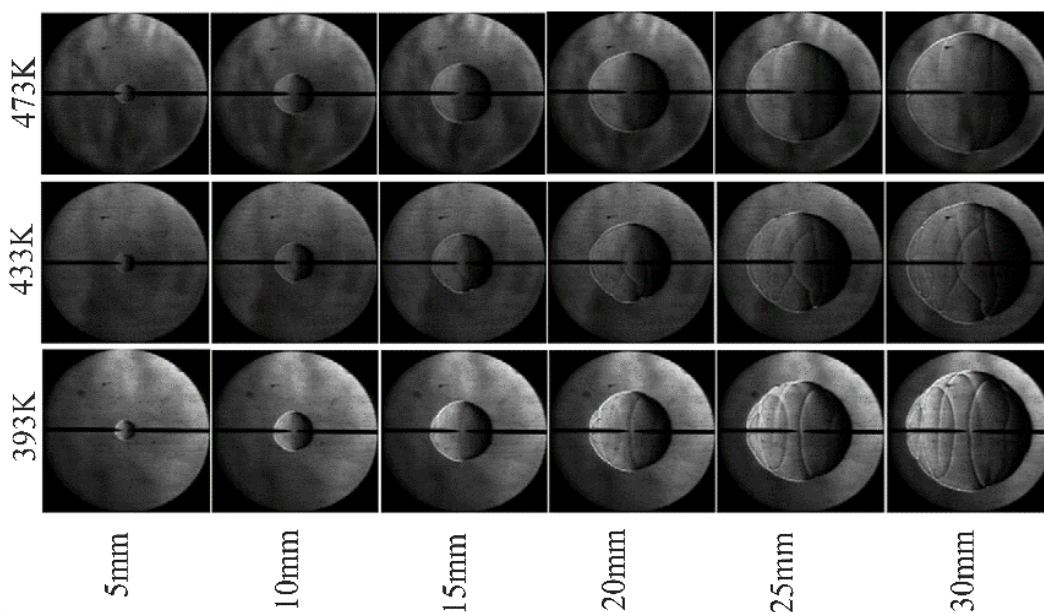

Fig 5. DMF-air mixture flame Schlieren images at three initial temperatures and the 1.5 equivalence ratio (Wu *et al.*, 2012)

Figure 4b depicts the flame development of a DMF/iso-octane (20/80) with four equivalence ratios (0.9, 1.1, 1.3, and 1.5). On this figure, it is easy to see the growing sphere inside the flame, with some cracks appearing on the front of the flame, especially those with a radius larger than 20mm for the equivalence ratio of 1.5 (Li *et al.*, 2012). This is because rich fuel blends such as DMF and iso-octane contain large amounts of heavy hydrocarbons. This phenomenon is also consistent with the conclusion that the Markstein length is negative and less variable. In Figures 4a and 4b, some cracks can also be seen on the flame front, even with changes in initial temperature and pressure (Wu *et al.*, 2012). In Figure 5, cracks can be seen in flames with a radius greater than 20 mm. When with increasing initial temperature, the occurrence of cracks tends to decrease due to the proportional relationship between Markstein length and initial temperature. However, at an initial pressure of 0.10 and 0.25 MPa and an equivalent ratio of 1.2, the flame front is quite smooth and has no cracks even when the flame radius is larger than 30 mm (Wu *et al.*, 2012). In addition, cracks appeared on the flame front with a pressure of 0.5 MPa. For flames with a radius of 30 mm or more, the cellular structures of the cracks can be observed under the same conditions (Nayak and Mishra, 2017). Importantly, the main factor affecting the flame structure is the diffusive-thermal-hydrodynamic instability. Thus, when increasing the initial pressure, both the flame thickness and Markstein length decrease. Figure 6a more clearly illustrates the schlieren images of DMF, MF, and iso-octane at the equilibrium equivalent ratio when studying the OH distribution and flame propagation (Ma et al., 2014b). At 350°CA, the flame velocity of DMF is lower than that of MF but is higher by 3.6 m/s compared to iso-octane. This lead to more growth of DMF heat release rate compared to iso-octane. In the case of higher IMEP, this difference is more obvious. Besides, many studies also focus on the analysis of OH-LIF data. The results show that the peak OH area value of DMF is about 10% higher than that of iso-octane. This suggests that compared to iso-octane, the combustion temperature of DMF is higher as shown by the flame image of the brighter DMF (Ma *et al.*, 2014b)(Bui *et al.*, 2021). In addition, Gillespie (Gillespie, 2014) conducted experiments to measure the LBV of DMF and MF by applying a flat flame burner. Experiments were conducted with a temperature in the range of 298K-398K, a pressure of 1 atm, the equivalent ratio varying from 0.55 to 1.65. The results of this study indicated that the LBV of the DMF peaked at the equivalent ratio of 1.1. In addition, it can be seen that the LBV of MF is higher than that of DMF at the maximum point of about 18 cm/s. However, it is special that at the higher temperature of 473K, the LBV of DMF is almost equivalent to that of MF. Meanwhile, at the lower temperature of 300K, the LBV of DMF50-I50 (50% DMF and 50% iso-octane by volume) was found to be lowest at all equivalent ratios. When adding DMF to the isooctane/air mixture, there was no significant change in the thermal diffusion of the unburnt gas mixture. Compared with the LBV of I100 (100% iso-octane), the LBV of the DMF50-I50 blend increased by about 5% under stoichiometric conditions. The cause of this increase may be due to an increase in the H molar fraction in the laminar flame. However, in the case where the variation

range of the equivalence ratio (Φ) is $0.6 \leq (\Phi) \leq 0.85$, the addition of DMF to iso-octane does not seem to affect LBV. More specifically, the above studies have also shown that the DMF30-I70 mixture can suppress the subzero temperature coefficient of iso-octane. This is a very useful finding, showing the use of a DMF/iso-octane mixture for SI engines without modification (Bhattacharya and Datta, 2019)(Vo *et al.*, 2020). Figures 6b depicts the flame profile of DMF relative to ethanol and gasoline with time progression at equilibrium equivalent ratios. On these figures, it can be seen that the LBV of ethanol is the highest of all the test fuels (including gasoline, ethanol, and DMF) at all initial temperature values. At 323K, the LBV peak value of gasoline is only 43 cm/s, while that of ethanol is 56 cm/s. The temperature reached 50°C, the LBV of ethanol was 56÷64 cm/s, while the LBV of DMF was 40÷49 cm/s (Tian *et al.*, 2010)(Thu and Anh, 2017). Obviously, ethanol has a very significant role in the rapid combustion mechanism, which is closely related to LBV and burning intensity. Recent literature has revealed significant differences in the LBVs of DMF and ethanol at a maximum dilution of 30% in internal combustion engines with an equivalent ratio range of about 0.9÷1.2. At 393K, the LBV of DMF and gasoline are pretty similar at low equivalence ratios. However, when the equivalence ratio is changed from 0.9 to 1.1 (this equivalence ratio is considered typical of gasoline engine operating conditions), the LBV of the DMF and the gasoline are about 10% different (Kumar and Kumar, 2021).

Sahu et al (Sahu *et al.*, 2020) conducted a study on the oxidation response of DMF when loading different fuels (X_F of 0.24, X_F of 0.14) with experiments performed in a counterflow diffusion flame burner. This work has shown that the formation of the 5-methyl-2 furanylmethyl radical is mainly caused by the abstraction of the reactive H atom from the CH_3 group. Approximately 65% of DMFs have undergone this abstraction reaction. The importance of CH_3 and H in the H atom separation reaction is reduced but that of C_5H_5 is increased in the case of X_F of 0.24. After that, the methyl alkylation was found to play a key role in transforming the intermediates to 2-methyl-5 ethylfuran or forming 2-keto-4,5hexadiene-3-yl from ß-scission, in which the ß-scission pathway dominated for X_F=0.14 case (Sauer *et al.*, 2021). Moreover, they detected that the H-atom addition to the ring-opening reaction was the second dominant pathway in consuming DMF aiming to produce hex-4-ene-2-one-3-yl, which was then converted into MF via the isomerisation process. To contribute to DMF consumption when forming CH_2=CH-CH=CH_2 and CH_3CO, the biomolecular reaction pathway with H atom has also been explored and published by previous studies. Another method for consuming DMF is to add an OH radical to the C2 atom of the furan ring yielding 2,5-dimethyl-2-hydroxyfuryl-3. As a result, a total mass of about 14% DMF was consumed by the above-mentioned two pathways for $X_F = 0.14$. However, the flame image shows a higher increased strain rate in the case of X_F=0.24, caused by the very significant contribution of the individual pathways. This is due to the influence of the equivalent ratios and mixing ratios of the DMF on the flame.
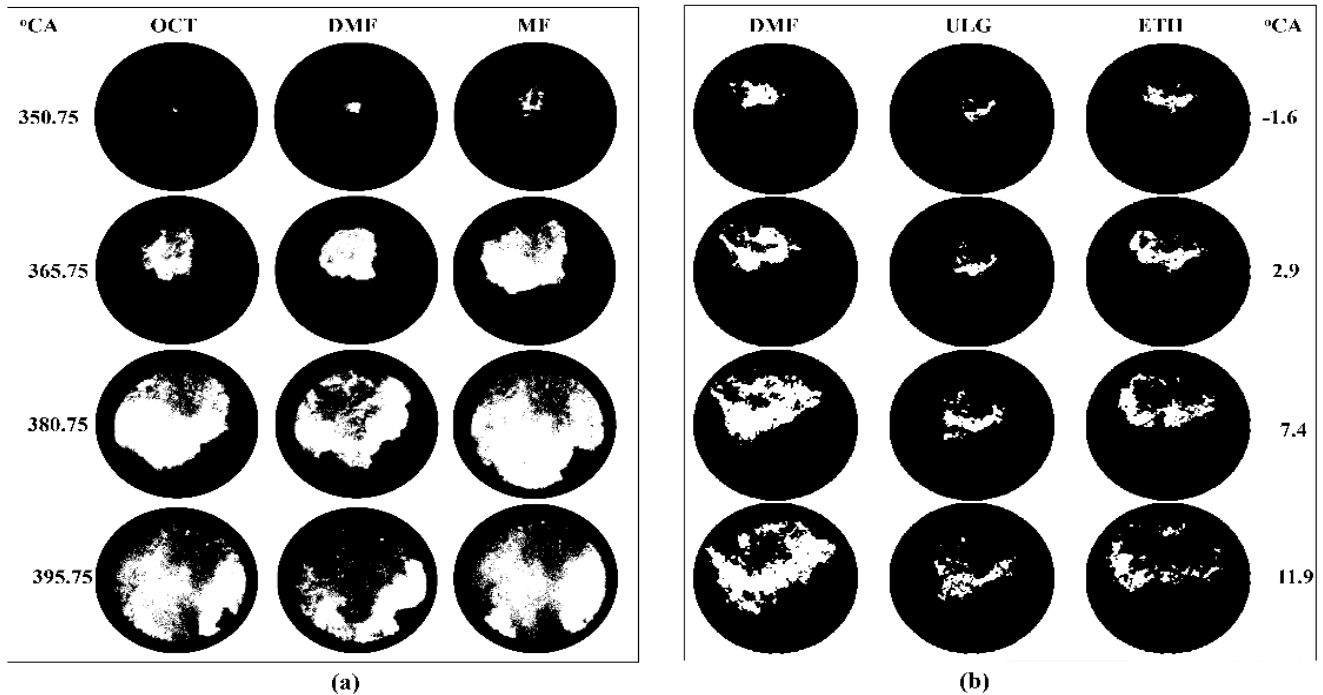
Fig 6. The comparison on chronological schlieren images of DMF with fuels; (a) - The flame images of MF, DMF, and iso-octane (Ma *et al*., 2014b); (b)(d) - Flame images of ethanol, gasoline, and DMF at IMEP 3bar (Tian *et al*., 2010).
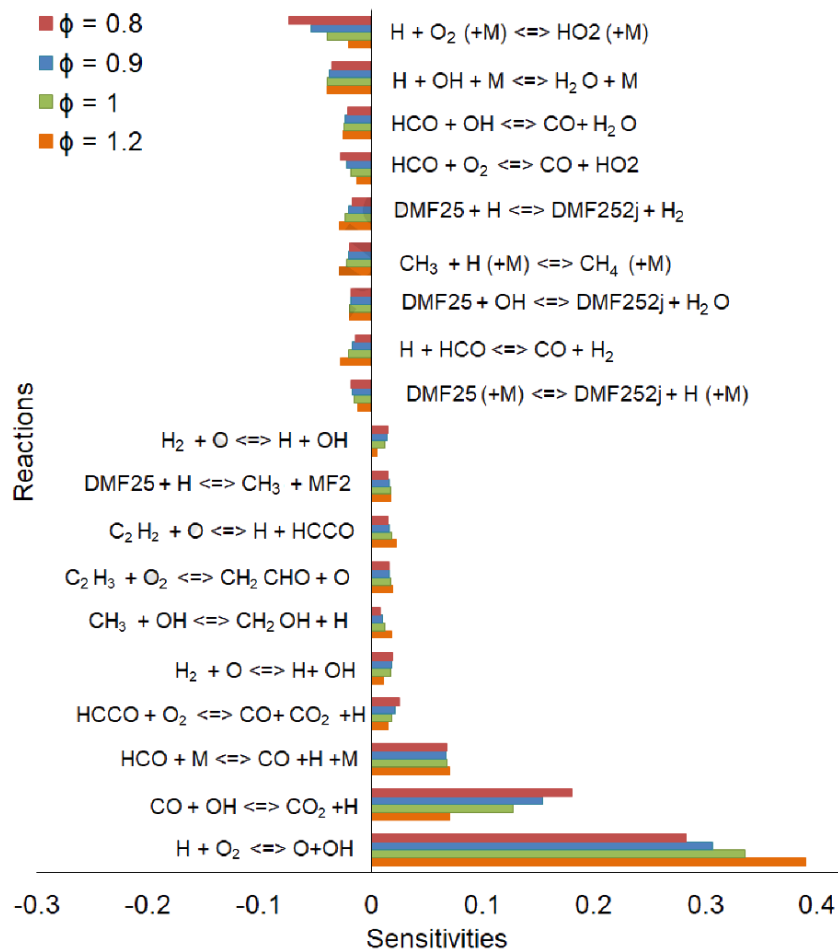

Fig 7. Sensitivity analysis on LBV of DMF-air mixture at different equivalence ratios, at 393K and 1 atm (Roy *et al*., 2019)

Interestingly, the reaction of H atom iso-addition to the DMF producing MF was determined to be an important contributor to the DMF consumption in the case of an uncompressed flame first (Togbé *et al.*, 2014), showing approximately approx. 8.7% and 6.1% for the case $X_F = 0.14$ and $X_F = 0.24$. Some works show that about 60% of DMF consumption is due to H-atom abstraction reactions as well as small hydrocarbon reactions, and thus significantly affects LBV even with blending cases. The effect of the H atom abstraction mechanism on LBV was determined by product sensitivity analysis. The analysis results show that, while C_5H_5 contributes only about 6.4% to DMF consumption, the CH_3 radical plays a dominant role in the H atom abstraction reaction (about 44%) (Tajuelo *et al.*, 2021)(Tran *et al.*, 2020). In this regard, Li et al. (Li *et al.*, 2022), Sahu et al (Sahu *et al.*, 2020) performed a sensitivity analysis of LBV to DMF at different equivalence ratios ($\Phi = 0.8 \div 1.2$) at a temperature of 393 K and a pressure of 1 atm. Figure 7 depicts the results of the analysis of the sensitivity of LBV to DMF with the change of the equivalence ratios.

It can be easily seen that the most sensitive reaction at all equivalence ratios is the forward reaction $H+O_2 \rightarrow O+OH$ (Figure 7). The next two sensitization reactions include $HCO+M \rightarrow CO+H+M$ and $CO+OH \rightarrow CO_2+H$. In addition, studies have also discovered a few reactions that can cause adverse effects on LBV, such as the reactions $H+OH+M \rightarrow H_2O+M$ and $H+O_2(+M) \rightarrow HO_2(+M)$. Clearly, the most important reactions are the light hydrocarbon reaction and the reaction that separates the H atom from the CH3 radical via O2- or OH. Therefore, the carbon chain branching reactions, thereby increasing the combustion rate, are caused by the reactions that separate the H atom from the CH3 group such as $C_2H_3+O_2 \rightarrow CH_2CHO+H$ and $C_2H_2+O \rightarrow H+HCCO$ (Roy *et al.*, 2019)(Vinayagam *et al.*, 2021). In particular, compared with the case of lower equivalence ratios, the reaction of abstracting the H atom ($CH_3+OH \rightarrow CH_2OH+H$) by the OH radical at a higher equivalence ratio was revealed to be more significant. At higher equivalence ratios, studies have found highly sensitive reactions of the H atom to the CH_3 group. In addition, compared with the reaction occurring in a lower equivalence ratio, the C-C chain branching reaction in the case of a high equivalence ratio has greater sensitivity. In case of a higher equivalence ratio will lead to larger cracks on the flame front (Giustini *et al.*, 2021). Sahu et al (Sahu *et al.*, 2020) also conducted similar studies for different fuel loads. Research results have also shown that the positive sensitivity for both cases reaches the maximum value with $X_F = 0.24$ and $X_F = 0.14$ is the positive sense of branched CC chains reacting like $H+O_2 \rightarrow OH+O$, and the next reaction $CO+OH \rightarrow CO_2+H$. But with higher fuel loading, the reactions $HCO(+ M) \rightarrow H+CO(+ M)$ and $H+O_2(+ M) \rightarrow HO_2(+ M)$ are considered as the dominant role (L. Zhang *et al.*, 2020).

3.2. Flame instabilities

Generally, flame surface instabilities are divided into three categories: buoyancy instability, thermal-diffusion instability, and Darrieus-Landau instability (also known as hydrodynamic instability) (Yin and Yan, 2016). However, the studies mentioned above all confirmed that because the LBV of the DMF is very high, the thermal-diffusion instability and hydrodynamics play an important role in the flame instability of the DMF. The combination of the effects of unequal diffusivity and pure curvature instability results in diffusive-thermal instability. This combination is represented via two parameters such as Markstein length or Lewis number. Besides, an important factor to determine the presence of unstable flame during propagation is the uneven deformation of the flame surface (Konnov *et al.*, 2018)(Xie and Li, 2019). The hydrodynamic instability of the flame is considered to be intrinsic instability, which is caused by the density jumping over the front of the flame. Two parameters control flame instability: flame density ratio and flame density (Dung and Anh, 2020). Typically, the cause of the hydrodynamic instability of the flame can be a decrease in the thickness of the flame or an increase in its density (Jomaas *et al.*, 2007)(Wu *et al.*, 2013). Initial factors such as pressure, temperature, fuel characteristics, or diluent concentration show that they all have different effects on flame instability when using DMF as a fuel. An increase in pressure will cause a decrease in flame enduring nature because of a decrease in thermal steady diffusion, thereby increasing hydrodynamic changeability. Most of the studies mentioned above confirm this. In addition, the flame changeability at high pressure also shows a significant growth according to the rise in the equivalence ratio due to the influence of heavy hydrocarbons such as DMF. This phenomenon can also be found even at atmospheric pressure in some cases. However, the overall stability will be improved as the initial temperature is increased, resulting in significantly increased thermal diffusion stability. In the case of the addition of diluent, the overall flame instability will be limited due to the reduced combustion temperature as well as the reduced reaction rate. In comparasion with ethanol and gasoline, the flame instability of DMF also tends to be higher. Besides, in the case where the equivalence ratio increases from 0.9 to 1.5, the tendency of the flame to be unstable of the mixture of DMF and iso-octane also increases. Because of the unclear effect of temperature on the Markstein length, the effect of the equivalence ratio on flame instability for other DMF mixtures is different. Sahu et al. (Sahu *et al.*, 2020) conducted a study based on both experimental and simulation which aimed to evaluate the quenching characteristic of DMF compared with MF in the case of adding iso-octane and N_2 under upstream diffuse flame conditions at 1 bar. As the fuel concentration increases, the extinction limitations also increase (Bui *et al.*, 2020). Thus, the work also reported on the extinction resistance ability of the fuel in the order DMF < isooctane < MF. The cause of the increase in the low fuel concentration shutdown limit is the mixing of iso-octane with DMF. However, at higher mixing concentrations, the effect of the blending ratio decreased. The separation of the hydrogen atom from the DMF molecular structure is considered to be an inevitable result of the fuel consumption pathway in the DMF flame. The role of C_5H_5 for the abstraction of the H atom in the DMF-air flame increases with increasing fuel load. Thus, the consistency of DMF combustion under different conditions has been confirmed by the above works, in which the above factors are said to significantly influence on the combustion behavior of DMF in the cylinder. Li et al. (Li *et al.*, 2012) also evaluated the effect

of the dilution ratio on the effective Lewis number (Leeff) in different equivalence ratios. At different equivalence ratios, Leeff's tendency to change is different. In the case of equivalent ratio = 0.9 (fuel-lean condition), Leeff decreases with increasing dilution ratio. On the other hand, the dilution ratio has a negligible effect on Leeff in the case of near-measured or slightly fuel-rich conditions. However, in the fuel-rich condition (equivalence ratio = 1.5), Leeff increased slightly with the increase of the dilution ratio. Figure 8 depicts the factors affecting flame instability.

In Figure 8, it can be seen that at an equivalent ratio and a certain dilution ratio, as the DMF mixing ratio increases (X_D), Leeff decreases. This suggests that when adding DMF to iso-octane, thermal diffusion instability tends to develop. Furthermore, the initial pressure had a negligible effect on the density ratio (Figure 9), while the flame thickness tended to decrease with increasing initial pressure (Wu *et al*., 2011)(Sahu *et al*., 2019). This is because of the smaller degree of Zeldovich number's variation (Ze) with the pressure compared with the flame thickness (Egolfopoulos *et al*., 2014). So, in the case of different initial pressures, the change of Le$_{eff}$ and the thickness of the flame dominated the change in the Markstein length. It can be seen that when Le$_{eff}$ < 1, then Markstein (L_b) < 0, and when Le$_{eff}$ > 1, the length of Markstein (L_b) > 0, corresponding to the case of flame propagation extending outward. Cell growth was no longer extinguished with the flame spreading outward and the elongation rate gradually decreased. Simultaneously, over the entire surface of the flame, cellular structures appeared almost instantaneously. The flame radius reaches a critical value at this critical moment. Whereas, the critical radius is standardized through the laminar flame thickness (which is represented by the Peclet-number). Besides that, during the immediate transition to cellularity, diffusion-thermal and hydrodynamic instability play an important role (Jomaas *et al*.,

2007)(Law *et al*., 2005). According to the theory of asymptotic, the Markstein length has been found to depend on the fuel Lewis number in a lean and the rich mixture, it depends on the oxidant (Williams, 2018). Therefore, the Markstein length is increased by the growth of the equivalence ratio of the lower-hydrocarbons/air mixture. In contrast, in the case of heavy hydrocarbons, the Markstein length decreases with the increase of the equivalence ratio (Giannakopoulos *et al*., 2015). Indeed, as the equivalence ratio increases, the Markstein length will decrease because DMF is a heavy hydrocarbon fuel. The relationship between the Markstein lengths of D20/air mixture and the different equivalence ratios under different initial pressures and the different initial temperatures (Dong *et al*., 2019)(Simsek *et al*., 2021). It is clear that, as the equivalence ratio increases, the Markstein length decreases under all conditions. On the other hand, it can be seen that the trend of its change in the two cases of pressure and temperature is different. The Markstein length increases with decreasing initial pressure or increasing temperature (Wu *et al*., 2012)(Wu *et al*., 2011).

Thus, through the results of the studies presented above, it can be confirmed that the flame tension rate has not significantly affected the spread of the flame under the higher initial pressure and the lower initial temperature. This results in a less stable flame of the D20/air mixture, especially in the cases of rich fuels. Malaton et al proposed a theory of the formation of a wrinkly flame stemming from the interaction of thermal instability and diffusion hydrodynamics. This can cause a large increase in the areas of the reaction, especially in the case of rich and heavy hydrocarbon fuels such as DMF (Tang *et al*., 2014)(Liu *et al*., 2018). In general, the characteristics of a cascade flame are given in the table below (Table 3).
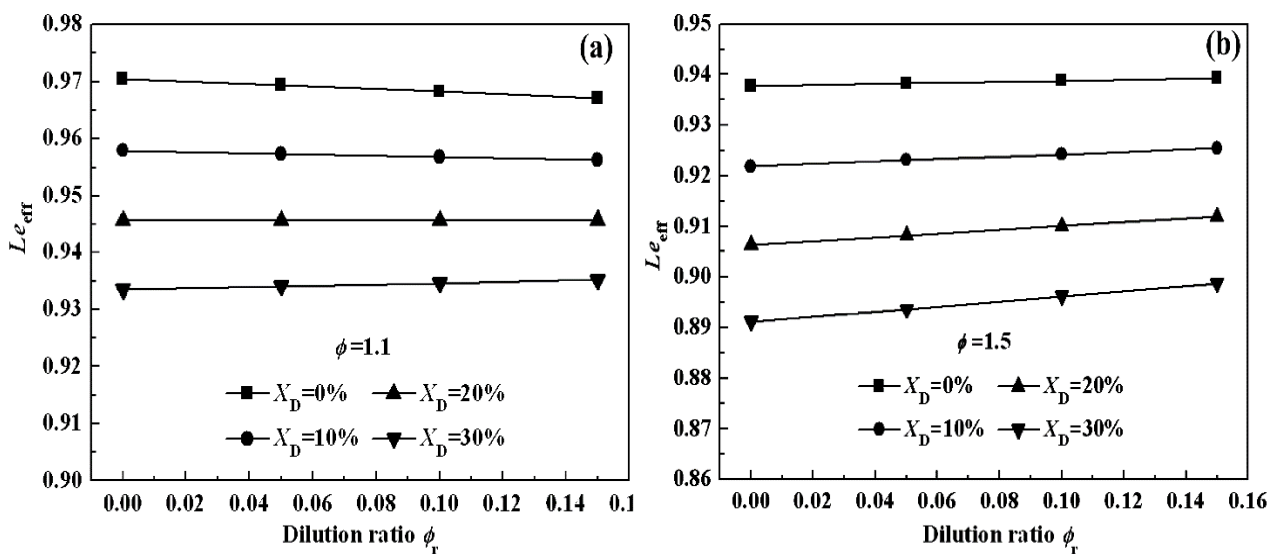

Fig 8. Relationship between equivalence ratios (φ) and Lewis number (Le$_{eff}$) for different ratios of DMF (Li *et al*., 2012)
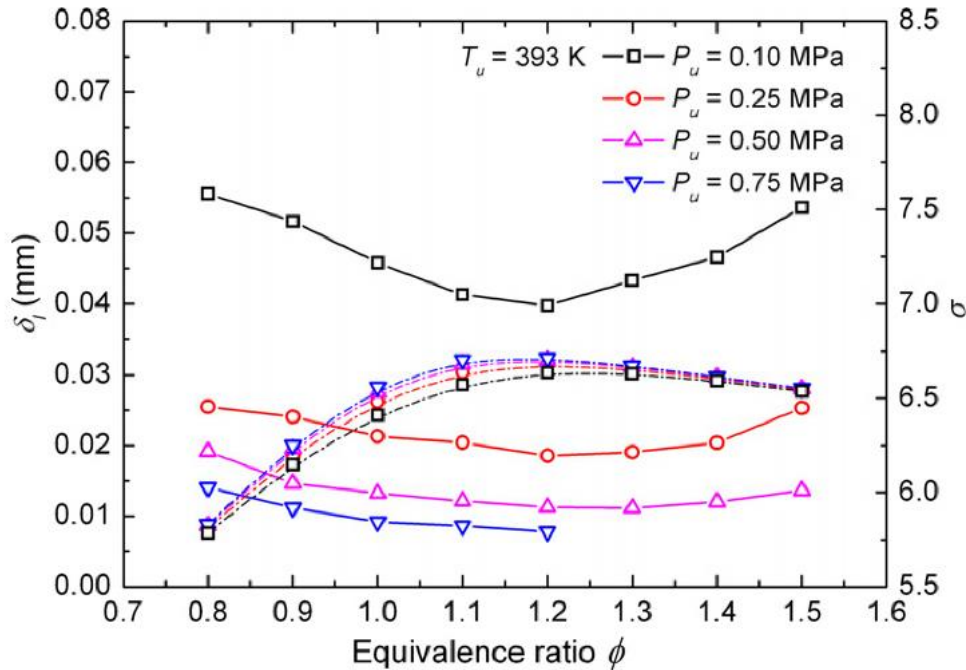
Fig 9. The correlation of the flame thickness (δ_l)/density ratio (σ) with equivalence ratios at four pressures (Wu *et al.*, 2011)

4. Challenges and future directions

The potential for the production of DMF is enormous because the raw materials for biorefineries derived from biomass are diverse and abundant. Recent advances in catalytic technology can accelerate the conversion of carbohydrate-like materials into furan-based fuels such as DMF (Onlamnao *et al.*, 2020)(Pandey *et al.*, 2022)(Guo *et al.*, 2020)(Buchori *et al.*, 2020). However, the achievements of conversion technology still do not mask the challenges of biomass pretreatment such as reactor selection, catalyst type, optimization of reaction conditions, and recovery solutions for by-product lines (Chiang *et al.*, 2020)(Aghaei *et al.*, 2020)(ZuoHua *et al.*, 2021). Another problem arises from the selection of feedstocks because related factors such as availability, ingredients, and cost determine the effectiveness of the circular economy transition (Le *et al.*, 2021). However, with a stronger sustainable and renewable energy transition strategy, sustainable energy development and decarbonization policies (Thomas *et al.*, 2021)(Bogdanov *et al.*, 2021) should be integrated with DMF production plants. Accordingly, renewable resources such as biomass, wind energy, and solar energy need to be utilized more optimally (Naqash *et al.*, 2021)(Dong *et al.*, 2021)(Pham *et al.*, 2021)(Atabani *et al.*, 2021) and deeply integrated Internet of Things technology achievements with long-term strategies (vom Lehn *et al.*, 2021)(Balasubramaniam *et al.*, 2021)(Simsek *et al.*, 2021).

Last but not least, this work is very useful as a premise for further studies on the application of DMF to engines in practice (Aykut and Sandro, 2021)(Bui *et al.*, 2021), and at the same time contributes to the development of high-performance catalytic systems and low-cost manufacturing processes. Most notably, DMF is considered as a potential furan derivative to improve combustion characteristics and reduce negative emissions from SI engines (Balasubramanian *et al.*, 2021) (Engel *et al.*, 2021) compared to ethanol and gasoline (Ya *et al.*, 2020)(Tran *et al.*, 2021). In addition, the advantages of stratified flame characteristics may open up potential applications of furan-based fuels for efficient applications in CI engines (Li *et al.*, 2021)(Sandro and Viet, 2020)(Alexandrino, 2020)(Ölçer and Nižetić, 2021). In short, a bright prospect to wake up the DMF giant is entirely possible in the coming decades.

Other challenges that cannot be ignored when using biofuels would come from the effects of properties such as viscosity, density, and vaporization on engine stability and durability (Hoang, 2019)(Tham *et al.*, 2019)(Gupta and Agarwal, 2021). Therefore, phenomena such as spray characteristics (Hoang, 2018), combustion chamber deposit formation (Le *et al.*, 2019)(Reddy and Nanthagopal, 2021)(Anh and Anh, 2019), or lubricant degradation (Ashok *et al.*, 2020)(Pham and Hoang, 2019) when using furan-based fuels in the future need to be further considered. In addition, the problem of corrosion of parts in the fuel system and combustion chamber also needs to be thoroughly investigated when using DMF fuel for internal combustion engines (Tabatabaei and Aghbashlo, 2020). More interesting, several new solutions that can be combined additives with biofuels to reduce emissions and engine durability concerns have been proposed recently such as the addition of metal nanoparticles (Hoang, 2021)(Murugesan *et al.*, 2021)(Norhafana *et al.*, 2018) and carbon nanoparticles (Atarod *et al.*, 2021)(Simsek *et al.*, 2021) to biodiesel fuel. In summary, although DMF holds within its great potential to become a promising alternative fuel, the above-mentioned obstacles and challenges need to be addressed as soon as possible before commercial use can be made.

Table 3
Laminar flame parameters in different conditions

Fuel	Conditions Equivalence ratios (Φ)	Temperature (K)	Pressure (atm)	Laminar flame parameters	Ref
Gasoline (G)-DMF-Ethanol (E)	0.8; 1.0, 1.3; 1.5; 1.8;	122; 167; 212	0.987	• ↔ S_n with ~ temperature; DMF & G peak S_n = 3 m/s; E peak S_n = 3.75 m/s; • ↔ LBV with ~ temperature; peak LBV comparison: E > G > DMF; peak LBV at equivalence ratios 1.1÷1.2; • ~ L_b with ~ temperatures; L_b comparison: E > G ≈ DMF, temperature at 122K; G > E > DMF at 167K; at 212K , ~ L_b for all experimental fuels;	(Tian *et al.*, 2010)
DMF, D10, D20, D30	0.9÷1.5	393	1	• ↑ S_n with ↑ DMF ratio in blends; ~ S_n with ↑ equivalence ratios; • ↑σ with ↑ DMF ratio in blends; ~ σ with ↑ equivalence ratios; σ min at equivalence ratio 0.9 & σ max at equivalence ratio 1.1; • ↓ δ_l with ↑ DMF ratio in blends; ~ δ_l with ↑ equivalence ratios; δ_l min at equivalence ratio 1.1 & δ_l max at equivalence ratio 1.5; • ↓ Le_{eff} with ↑ DMF ratio in blends; ↓ Le_{eff} with ↑ equivalence ratios;	(Li *et al.*, 2012)
D20 (20%DMF +80% iso-octane)	0.9÷1.5	393; 433; 473	0.987; 2.467; 4.935	• ↓ S_n with ↓ equivalence ratios at 393K & 0.987 atm; • ↓ LBV with ↑ pressure at 393K & various equivalence ratios, peak LBV at equivalence ratio 1.2; ↓ LBV with ↓ temperature at 0.987 atm and various equivalence ratios, peak LBV at equivalence ratio1.3; • ↑ LBF with ↑ pressure at 393K; ↑ LBF with ↑ temperature at 0.987 atm; • ↑ L_b, ↓ σ, ↑δ_l with ↓ pressure, temperature and various equivalence ratios;	(Wu *et al.*, 2012)
DMF	0.6÷1.6	298; 358	1÷7.5	• peak LBV at equivalence ratio 1.1; ↓ LBV with ↑ pressure, • peak LBV at equivalence ratio 1.1; ↓ LBV with ↓temperature, • peak LBV at equivalence ratio 1.1; ↓ LBV with ↑ DMF ratios, peak LBV: iso-octane = 33 cm/s; 1/2DMF+1/2iso-octane = 36 cm/s, DMF = 38 cm/s,	(Somers *et al.*, 2013)
Pure iso-octane (100%)-1/2DMF+1/2iso-octane (in volume)-pure DMF	0.8; 1.0; 1.3; 1.5; 1.8	300	1		(Bhattacharya and Datta, 2019)
DMF	0.6÷1.6	298, 358, 393 , 458	1	• peak LBV at equivalence ratio 1.1; ↓ LBV with ↓ temperature, • ↓ S_n with ↑ pressure;	(Tian *et al.*, 2019)
DMF	0.8÷1.5	393	0.987; 2.467; 4.935; 7.402	• ↓ LBV with ↓ equivalence ratios with various pressure, peak LBV at 0.987 atm; ↓ LBV with ↑ pressure with various equivalence ratios, peak LBV at equivalence ratio 1.2; • ↑ LBF with ↑ pressure; peak LBF at equivalence ratio 1.2; • ↑ L_b, ↓ σ, ↑δ_l with ↓ pressure with various equivalence ratios; peak LBF at equivalence ratio 1.2;	(Wu *et al.*, 2011)
MF-DMF-iso-octane			4.441; 5.428 (IMEP)	• LBV comparison: - DMF ≈ iso-octane < MF at 4.441 atm IMEP; - iso-octane < DMF < at 5.428 atm IMEP; • ↑↓ LBV with ↑ equivalence ratios, LBV min at equivalence ratio 0.6, LBV max at equivalence ratio 1.0; • ↑ LBV with ↑ DMF ratios;	(Ma *et al.*, 2013)
DMF-Blends (DMF + iso-octane at various ratios of 5%-50%)	0.6÷1.4	393	1		(Roy *et al.*, 2019)

5. Conclusions

To be seen as an alternative second-generation biofuel in replacing traditional fuels when used in internal combustion engines, DMF has many advantages such as high-octane number, insoluble in water, high heating value, especially in mixing with traditional fuels in many different ratios. This paper presents an overview of the time evolution of the laminar flame characteristics. At the same time, its instability is also considered and analyzed based on the reaction diagrams and the molar fractional configuration of the species formed. The evaluation results show that the layered combustion rate of DMF is lower than that of ethanol but is almost equivalent to that of gasoline. By using the analysis method of product ratios and their molar fraction, the mechanism of changing the laminar combustion velocity of DMF according to different initial parameters was also meticulously analyzed. The

analysis results show that DMF is very suitable for use on spark-ignition engines.

Both theoretical research and experimental research needs to be conducted to collect and develop chemical knowledge to the root of the DMF reactions response under different conditions. In particular, studies on the estimated kinetic parameters of basis reaction steps were advised to refine to validate proposed reaction pathways more rigorously. Moreover, this work was believed to support the numerous global reactivity measurements that have been existing in the literature.

References

Ab Rasid, N.S., Shamjuddin, A., Rahman, A.Z.A., Amin, N.A.S., 2021. Recent advances in green pre-treatment methods of lignocellulosic biomass for enhanced biofuel production. J. Clean. Prod. 129038.

Abyaz, A., Afra, E., Saraeyan, A., 2020. Improving technical parameters of biofuel briquettes using cellulosic binders. Energy Sources, Part A Recover. Util. Environ. Eff. 1–12.

Aghaei, A., Shahhosseini, S., Sobati, M.A., 2020. Regeneration of different extractive solvents for the oxidative desulfurization process: An experimental investigation. Process Saf. Environ. Prot. 139, 191–200.

Al-Tawaha, A., Pham, M.T., Le, A.T., Dong, V.H., Le, V.V., 2018. Measurement and prediction of the density and viscosity of biodiesel blends. Int. J. Technol. 5, 1015–1026.

Alami, A.H., Tawalbeh, M., Alasad, S., Ali, M., Alshamsi, M., Aljaghoub, H., 2021. Cultivation of Nannochloropsis algae for simultaneous biomass applications and carbon dioxide capture. Energy Sources, Part A Recover. Util. Environ. Eff. 1–12.

Alexandrino, K., 2020. Comprehensive Review of the Impact of 2, 5-Dimethylfuran and 2-Methylfuran on Soot Emissions: Experiments in Diesel Engines and at Laboratory-Scale. Energy & Fuels.

An, H., Yang, W.M., Maghbouli, A., Chou, S.K., Chua, K.J., 2013. Detailed physical properties prediction of pure methyl esters for biodiesel combustion modeling. Appl. Energy 102, 647–656.

Anh, L.T., Anh, H.T., 2019. Trilateral correlation of spray characteristics, combustion parameters, and deposit formation in the injector hole of a diesel engine running on preheated Jatropha oil and fossil diesel fuel. Biofuel Res. J. 6, 909–919. https://doi.org/10.18331/BRJ2019.6.1.2

Arias-Fernández, I., Romero Gómez, M., Romero Gómez, J., López-González, L.M., 2020. Generation of H2 on board LNG vessels for consumption in the propulsion system. Polish Marit. Res. 27, 83–95.

Ashok, B., Nanthagopal, K., Chyuan, O.H., Le, P.T.K., Raje, N., Raj, A., Karthickeyan, V., Tamilvanan, A., 2020. Multi-functional fuel additive as a combustion catalyst for diesel and biodiesel in CI engine characteristics. Fuel 278, 118250.

Atabani, A.E., Tyagi, V.K., Fongaro, G., Treichel, H., Pugazhendhi, A., 2021. Integrated biorefineries, circular bio-economy, and valorization of organic waste streams with respect to bio-products.

Atarod, P., Khlaife, E., Aghbashlo, M., Tabatabaei, M., Hoang, A.T., Mobli, H., Nadian, M.H., Hosseinzadeh-Bandbafha, H., Mohammadi, P., Shojaei, T.R., 2021. Soft computing-based modeling and emission control/reduction of a diesel engine fueled with carbon nanoparticle-dosed water/diesel emulsion fuel. J. Hazard. Mater. 407, 124369.

Aykut, Ö.I., Sandro, N., 2021. 2,5-Dimethylfuran (DMF) as a promising biofuel for the spark ignition engine application: A comparative analysis and review. Fuel 285, 119140. https://doi.org/10.1016/j.fuel.2020.119140

Badawy, T., Williamson, J., Xu, H., 2016. Laminar burning characteristics of ethyl propionate, ethyl butyrate, ethyl acetate, gasoline and ethanol fuels. Fuel 183, 627–640.

Balasubramaniam, D., Nguyen, H.P., Le, P.Q.H., Pham, V.V., Nguyen, X.P., Hoang, A.-T., 2021. Application of the Internet of Things in 3E (efficiency, economy, and environment) factor-based energy management as smart and sustainable strategy. Energy Sources, Part A Recover. Util. Environ. Eff. 1–23.

Balasubramanian, D., Konur, O., Nguyen, D.C., Tran, V.N., Bui, T.T., 2021. Characteristics of PM and soot emissions of internal combustion engines running on biomass-derived DMF biofuel: A review. Energy Sources, Part A Recover. Util. Environ. Eff.

Bamisile, O., Dagbasi, M., Huang, Q., Williams, N., Ruwa, T., Babatunde, A., Kemena, A.D., 2020. A biomass-integrated comprehensive energy system: thermodynamics assessment and performance comparison of sugarcane bagasse and rice husk as input source. Energy Sources, Part A Recover. Util. Environ. Eff. 1–18.

Benson, R.S., Whitehouse, N.D., 2013. Internal combustion engines: a detailed introduction to the thermodynamics of spark and compression ignition engines, their design and development. Elsevier.

Bhattacharya, A., Datta, A., 2019. Effects of blending 2, 5-dimethylfuran on the laminar burning velocity and ignition delay time of isooctane/air mixture. Combust. Theory Model. 23, 105–126.

Binder, J.B., Raines, R.T., 2009. Simple chemical transformation of lignocellulosic biomass into furans for fuels and chemicals. J. Am. Chem. Soc. 131, 1979–1985.

Bogdanov, D., Ram, M., Aghahosseini, A., Gulagi, A., Oyewo, A.S., Child, M., Caldera, U., Sadovskaia, K., Farfan, J., Barbosa, L.D.S.N.S., 2021. Low-cost renewable electricity as the key driver of the global energy transition towards sustainability. Energy 227, 120467.

Bohre, A., Dutta, S., Saha, B., Abu-Omar, M.M., 2015. Upgrading furfurals to drop-in biofuels: An overview. ACS Sustain. Chem. Eng. 3, 1263–1277.

Bradley, D., Lawes, M., Liu, K., Verhelst, S., Woolley, R., 2007. Laminar burning velocities of lean hydrogen–air mixtures at pressures up to 1.0 MPa. Combust. Flame 149, 162–172.

Buchori, L., Djaeni, M., Ratnawati, R., Retnowati, D.S., Hadiyanto, H., Anggoro, D.D., 2020. Glycerolysis Using KF/CaO-MgO Catalyst: Optimisation and Reaction Kinetics. J. Teknol. 82.

Bui, T.M.T., Nguyen Thi, T.X., Vo, A.V., Bui, V.G., Nižetić, S., 2021. Hydrogen-Enriched Biogas Premixed Charge Combustion and Emissions in Direct Injection and Indirect Injection Diesel Dual Fueled Engines: A Comparative Study. J. Energy Resour. Technol. 143. https://doi.org/10.1115/1.4051574

Bui, T.T., Luu, H.Q., Konur, O., Huu, T., Pham, M.T., 2020. A review on ignition delay times of 2,5-Dimethylfuran. Energy Sources, Part A Recover. Util. Environ. Eff. 1–16. https://doi.org/10.1080/15567036.2020.1860163

Burke, M.P., Chen, Z., Ju, Y., Dryer, F.L., 2009. Effect of cylindrical confinement on the determination of laminar flame speeds using outwardly propagating flames. Combust. Flame 156, 771–779.

Cao, D.N., Luu, H.Q., Bui, V.G., Tran, T.T.H., 2020. Effects of injection pressure on the NOx and PM emission control of diesel engine: A review under the aspect of PCCI combustion condition. Energy Sources, Part A Recover. Util. Environ. Eff. 1–18.

Chan, D.N., 2018. Properties of DMF-fossil gasoline RON95 blends in the consideration as the alternative fuel. Int. J. Adv. Sci. Eng. Inf. Technol. 8, 2555–2560.

Chau MQ, Le V V, Al-Tawaha A, Pham V V (2020) A simulation research of heat transfers and chemical reactions in the fuel steam reformer using exhaust gas energy from motorcycle engine. J Mech Eng Res Dev 43:89–102.

Chau, M.Q., Nguyen, D.C., Hoang, A.T., Tran, Q.V., Pham, V.V., 2020. A Numeral Simulation Determining Optimal

Ignition Timing Advance of SI Engines Using 2.5-Dimethylfuran-Gasoline Blends. Int. J. Adv. Sci. Eng. Inf. Technol. 10, 1933–1938.

Chen, G., Shen, Y., Zhang, Q., Yao, M., Zheng, Z., Liu, H., 2013. Experimental study on combustion and emission characteristics of a diesel engine fueled with 2, 5-dimethylfuran–diesel, n-butanol–diesel and gasoline–diesel blends. Energy 54, 333–342.

Chen, N., Zhu, Z., Su, T., Liao, W., Deng, C., Ren, W., Zhao, Y., Lü, H., 2020. Catalytic hydrogenolysis of hydroxymethylfurfural to highly selective 2, 5-dimethylfuran over FeCoNi/h-BN catalyst. Chem. Eng. J. 381, 122755.

Chen, W.-H., Nižetić, S., Sirohi, R., Huang, Z., Luque, R., M.Papadopoulos, A., Sakthivel, R., Phuong Nguyen, X., 2021. Liquid hot water as sustainable biomass pretreatment technique for bioenergy production: A review. Bioresour. Technol. 126207. https://doi.org/10.1016/j.biortech.2021.126207

Chen, Z., Burke, M.P., Ju, Y., 2009. Effects of Lewis number and ignition energy on the determination of laminar flame speed using propagating spherical flames. Proc. Combust. Inst. 32, 1253–1260.

Cheng, C.K., Ong, H.C., Fattah, I.M.R., Chong, C.T., Sakthivel, R., Ok, Y.S., 2021. Progress on the lignocellulosic biomass pyrolysis for biofuel production toward environmental sustainability. Fuel Process. Technol. 223, 106997. https://doi.org/10.1016/j.fuproc.2021.106997

Chiang, Y., Bassas, H.N., Lively, R.P., Nair, S., 2020. Separation and Purification of 2, 5-Dimethylfuran: Process Design and Comparative Technoeconomic and Sustainability Evaluation of Simulated Moving Bed Adsorption and Conventional Distillation. ACS Sustain. Chem. Eng. 8, 12482–12492.

Chidambaram, M., Bell, A.T., 2010. A two-step approach for the catalytic conversion of glucose to 2, 5-dimethylfuran in ionic liquids. Green Chem. 12, 1253–1262.

Chong, C.T., Nizetic, S., Ong, H.C., Atabani, A.E., Pham, V.V., 2021. Acid-based lignocellulosic biomass biorefinery for bioenergy production: advantages, application constraints, and perspectives. J. Environ. Manage.

Christwardana, M., Hadiyanto, H., Motto, S.A., Sudarno, S., Haryani, K., 2020. Performance evaluation of yeast-assisted microalgal microbial fuel cells on bioremediation of cafeteria wastewater for electricity generation and microalgae biomass production. Biomass and Bioenergy 139, 105617. https://doi.org/10.1016/j.biombioe.2020.105617

Chu, H., Xiang, L., Nie, X., Ya, Y., Gu, M., Jiaqiang, E., 2020. Laminar burning velocity and pollutant emissions of the gasoline components and its surrogate fuels: A review. Fuel 269, 117451.

Daniel, R., Wang, C., Xu, H., Tian, G., 2012a. Split-injection strategies under full-load using DMF, a new biofuel candidate, compared to ethanol in a GDI engine. SAE Technical Paper.

Daniel, R., Wei, L., Xu, H., Wang, C., Wyszynski, M.L., Shuai, S., 2012b. Speciation of hydrocarbon and carbonyl emissions of 2, 5-dimethylfuran combustion in a DISI engine. Energy & fuels 26, 6661–6668.

Djokic, M., Carstensen, H.-H., Van Geem, K.M., Marin, G.B., 2013. The thermal decomposition of 2, 5-dimethylfuran. Proc. Combust. Inst. 34, 251–258.

Dong, V.H., Nguyen, X.P., Le, N.D., Pham, V.V., Huynh, T.T., 2021. Mission, challenges, and prospects of renewable energy development in Vietnam. Energy Sources, Part A Recover. Util. Environ. Eff. 1–13. https://doi.org/10.1080/15567036.2021.1965264

Dong, V.H., Tran, V.D., Le, A.T., 2019. An experimental analysis on physical properties and spray characteristics of an ultrasound-assisted emulsion of ultra-low-sulphur diesel and Jatropha-based biodiesel. J. Mar. Eng. Technol.

https://doi.org/10.1080/20464177.2019.1595355

Dung, V.T., Anh, H.T., 2020. Experimental Analysis on the Ultrasound-based Mixing Technique Applied to Ultra-low Sulphur Diesel and Bio-oils 9, 307–313.

Dutta, S., 2012. Deoxygenation of biomass-derived feedstocks: hurdles and opportunities. ChemSusChem 5, 2125–2127.

Dutta, S., De, S., Alam, M.I., Abu-Omar, M.M., Saha, B., 2012. Direct conversion of cellulose and lignocellulosic biomass into chemicals and biofuel with metal chloride catalysts. J. Catal. https://doi.org/10.1016/j.jcat.2011.12.017

Egolfopoulos, F.N., Hansen, N., Ju, Y., Kohse-Höinghaus, K., Law, C.K., Qi, F., 2014. Advances and challenges in laminar flame experiments and implications for combustion chemistry. Prog. Energy Combust. Sci. 43, 36–67.

Engel, D., I.Ölçer, A., Pham, V.V., Nayak, S.K., 2021. Biomass-derived 2,5-dimethylfuran as a promising alternative fuel: An application review on the compression and spark ignition engine. Fuel Process. Technol. https://doi.org/10.1016/j.fuproc.2020.106687

Feng, L., Li, X., Lin, Y., Liang, Y., Chen, Y., Zhou, W., 2020. Catalytic hydrogenation of 5-hydroxymethylfurfural to 2, 5-dimethylfuran over Ru based catalyst: Effects of process parameters on conversion and products selectivity. Renew. Energy 160, 261–268.

Fenton, J., 1998. Handbook of automotive powertrains and chassis design. Professional Engineering Publishing.

Ga Bui, V., Nižetić, S., Viet Pham, V., Tuan Le, A., Vang Le, V., 2021. Combustion and emission characteristics of spark and compression ignition engine fueled with 2,5-dimethylfuran (DMF): A comprehensive review. Fuel 288, 119757. https://doi.org/https://doi.org/10.1016/j.fuel.2020.119757

Galmiche, B., Halter, F., Foucher, F., 2012. Effects of high pressure, high temperature and dilution on laminar burning velocities and Markstein lengths of iso-octane/air mixtures. Combust. Flame 159, 3286–3299.

Geo, V.E., Thiyagarajan, S., Sonthalia, A., Prakash, T., Awad, S., Aloui, F., Pugazhendhi, A., 2021. CO2 reduction in a common rail direct injection engine using the combined effect of low carbon biofuels, hydrogen and a post combustion carbon capture system. Energy Sources, Part A Recover. Util. Environ. Eff. 1–20.

Giannakopoulos, G.K., Gatzoulis, A., Frouzakis, C.E., Matalon, M., Tomboulides, A.G., 2015. Consistent definitions of "Flame Displacement Speed" and "Markstein Length" for premixed flame propagation. Combust. Flame 162, 1249–1264.

Gillespie, F.R., 2014. An experimental and modelling study of the combustion of oxygenated hydrocarbons.

Giustini, A., Aschi, M., Park, H., Meloni, G., 2021. Theoretical and experimental study on the O (3 P)+ 2, 5-dimethylfuran reaction in the gas phase. Phys. Chem. Chem. Phys. 23, 19424–19434.

Guo, D., Liu, X., Cheng, F., Zhao, W., Wen, S., Xiang, Y., Xu, Q., Yu, N., Yin, D., 2020. Selective hydrogenolysis of 5-hydroxymethylfurfural to produce biofuel 2, 5-dimethylfuran over Ni/ZSM-5 catalysts. Fuel 274, 117853.

Gupta, J.G., Agarwal, A.K., 2021. Engine durability and lubricating oil tribology study of a biodiesel fuelled common rail direct injection medium-duty transportation diesel engine. Wear 486, 204104.

Hadiyanto, H., Halim, M.A.R., Muhammad, F., Soeprobowati, T.R., Sularto, S., 2021. Potential for Environmental Services Based on the Estimation of Reserved Carbon in the Mangunharjo Mangrove Ecosystem. Polish J. Environ. Stud. 30, 3545–3552.

Han, W., Tang, M., Li, J., Li, X., Wang, J., Zhou, L., Yang, Y., Wang, Y., Ge, H., 2020. Selective hydrogenolysis of 5-hydroxymethylfurfural to 2, 5-dimethylfuran catalyzed by ordered mesoporous alumina supported nickel-molybdenum sulfide catalysts. Appl. Catal. B Environ. 268,

118748.

Han, X., Wang, Z., Wang, S., Whiddon, R., He, Y., Lv, Y., Konnov, A.A., 2019. Parametrization of the temperature dependence of laminar burning velocity for methane and ethane flames. Fuel 239, 1028–1037.

Hoang, A.T., 2021. Combustion behavior, performance and emission characteristics of diesel engine fuelled with biodiesel containing cerium oxide nanoparticles: A review. Fuel Process. Technol. 218, 106840.

Hoang, A.T., 2019. Experimental study on spray and emission characteristics of a diesel engine fueled with preheated bio-oils and diesel fuel. Energy 171, 795–808. https://doi.org/10.1016/j.energy.2019.01.076

Hoang, A.T., 2018. Prediction of the density and viscosity of biodiesel and the influence of biodiesel properties on a diesel engine fuel supply system. J. Mar. Eng. Technol. 1–13. https://doi.org/10.1080/20464177.2018.1532734

Hu, B., Warczinski, L., Li, X., Lu, M., Bitzer, J., Heidelmann, M., Eckhard, T., Fu, Q., Schulwitz, J., Merko, M., 2020. Formic Acid-Assisted Selective Hydrogenolysis of 5-Hydroxymethylfurfural to 2, 5-Dimethylfuran over Bifunctional Pd Nanoparticles Supported on N-doped Mesoporous Carbon. Angew. Chemie Int. Ed.

Hu, L., Jiang, Y., Xu, Jiaxing, He, A., Wu, Z., Xu, Jiming, 2020. Chemocatalytic pathways for high-efficiency production of 2, 5-dimethylfuran from biomass-derived 5-hydroxymethylfurfural, in: Biomass, Biofuels, Biochemicals. Elsevier, pp. 377–394.

Huang, Z., Zhang, Y., Zeng, K., Liu, B., Wang, Q., Jiang, D., 2006. Measurements of laminar burning velocities for natural gas–hydrogen–air mixtures. Combust. Flame 146, 302–311.

Huynh, T.T., Nguyen, X.P., Le, A.T., Pham, V.V., 2021. COVID-19 and the Global Shift Progress to Clean Energy. J. Energy Resour. Technol. 143, 94701. https://doi.org/10.1115/1.4050779

İlçin, K., Altun, Ş., 2021. Effect of biodiesel addition in a blend of isopropanol-butanol-ethanol and diesel on combustion and emissions of a CRDI engine. Energy Sources, Part A Recover. Util. Environ. Eff. 1–13.

Jomaas, G., Law, C.K., Bechtold, J.K., 2007. On transition to cellularity in expanding spherical flames. J. Fluid Mech. 583, 1.

Kadarwati, S., Apriliani, E., Annisa, R.N., Jumaeri, J., Cahyono, E., Wahyuni, S., 2021. Esterification of Bio-Oil Produced from Sengon (Paraserianthes falcataria) Wood Using Indonesian Natural Zeolites. Int. J. Renew. Energy Dev. 10, 747–754.

Katagi, K.S., Kadam, N.S., Munnolli, R.S., Benni, S.D., 2021. Investigation on seed oil chemistry of Bauhinia racemosa for the production of liquid biofuel. Energy Sources, Part A Recover. Util. Environ. Eff. 1–13.

Klemeš, J.J., Jiang, P., Van Fan, Y., Bokhari, A., Wang, X.-C., 2021. COVID-19 pandemics Stage II–energy and environmental impacts of vaccination. Renew. Sustain. Energy Rev. 150, 111400.

Konnov, A.A., Mohammad, A., Kishore, V.R., Kim, N. Il, Prathap, C., Kumar, S., 2018. A comprehensive review of measurements and data analysis of laminar burning velocities for various fuel+ air mixtures. Prog. Energy Combust. Sci. 68, 197–267.

Kumar, L., Bharadvaja, N., 2020. A review on microalgae biofuel and biorefinery: challenges and way forward. Energy Sources, Part A Recover. Util. Environ. Eff. 1–24.

Kumar, R., Kumar, S., 2021. Formulation of a three-component gasoline surrogate model using laminar burning velocity data at elevated mixture temperatures. Fuel 306, 121581.

Law, C.K., 2010. Combustion physics. Cambridge university press.

Law, C.K., Jomaas, G., Bechtold, J.K., 2005. Cellular instabilities of expanding hydrogen/propane spherical flames at elevated pressures: theory and experiment. Proc. Combust. Inst. 30, 159–167.

Le Anh, T., Pham Van, V., Anh Hoang, T., 2019. A core correlation of spray characteristics, deposit formation, and combustion of a high-speed diesel engine fueled with Jatropha oil and diesel fuel. Fuel 244, 159–175. https://doi.org/10.1016/j.fuel.2019.02.009

Le, T.H., Huynh, T.T., Nguyen, X.P., Nguyen, T.K.T., 2021. An analysis and review on the global NO2 emission during lockdowns in COVID-19 period. Energy Sources, Part A Recover. Util. Environ. Eff. https://doi.org/10.1080/15567036.2021.1902431

Le, V.V., Hoang, T.A., 2017. The Performance of A Diesel Engine Fueled With Diesel Oil, Biodiesel and Preheated Coconut Oil. Int. J. Renew. Energy Dev. 6, 1.

Le, V.V., Nižetić, S., Ölçer, A.I., 2021. Flame Characteristics and Ignition Delay Times of 2,5-Dimethylfuran: A Systematic Review With Comparative Analysis. J. Energy Resour. Technol. 143. https://doi.org/10.1115/1.4048673

Li, Q., Fu, J., Wu, X., Tang, C., Huang, Z., 2012. Laminar flame speeds of DMF/iso-octane-air-N2/CO2 mixtures. Energy & fuels 26, 917–925.

Li, Y., Xu, W., Jiang, Y., Liew, K.M., 2022. Effects of diluents on laminar burning velocity and cellular instability of 2-methyltetrahydrofuran-air flames. Fuel 308, 121974.

Li, Ya, Xu, W., Jiang, Y., Liew, K.M., Qiu, R., 2021. Laminar burning velocities of 2-methyltetrahydrofuran at elevated pressures. Proc. Combust. Inst. 38, 2175–2183.

Li, Yuqiang, Zhao, J., Tang, W., Abubakar, S., Wu, G., Huang, J., 2021. Development and application of a practical diesel-n-butanol-PAH mechanism in engine combustion and emissions prediction. Energy Sources, Part A Recover. Util. Environ. Eff. 1–15.

Lifshitz, A., Tamburu, C., Shashua, R., 1998. Thermal decomposition of 2, 5-dimethylfuran. Experimental results and computer modeling. J. Phys. Chem. A 102, 10655–10670.

Lin, X., Li, M., Jian, Y., Huang, J., Yang, S., Li, H., 2021. One-pot domino conversion of biomass-derived furfural to γ-valerolactone with an in-situ formed bifunctional catalyst. Energy Sources, Part A Recover. Util. Environ. Eff. 1–17.

Liu, H., Wang, X., Zhang, D., Dong, F., Liu, X., Yang, Y., Huang, H., Wang, Y., Wang, Q., Zheng, Z., 2019. Investigation on Blending Effects of Gasoline Fuel with N-Butanol, DMF, and Ethanol on the Fuel Consumption and Harmful Emissions in a GDI Vehicle. Energies 12, 1845.

Liu, H., Zhang, P., Liu, X., Chen, B., Geng, C., Li, B., Wang, H., Li, Z., Yao, M., 2018. Laser diagnostics and chemical kinetic analysis of PAHs and soot in co-flow partially premixed flames using diesel surrogate and oxygenated additives of n-butanol and DMF. Combust. Flame 188, 129–141.

Ma'As, M.F., Ghazali, H.M., Chieng, S., 2020. Bioethanol production from Brewer's rice by Saccharomyces cerevisiae and Zymomonas mobilis: evaluation of process kinetics and performance. Energy Sources, Part A Recover. Util. Environ. Eff. 1–14.

Ma, X., Jiang, C., Xu, H., Ding, H., Shuai, S., 2014a. Laminar burning characteristics of 2-methylfuran and isooctane blend fuels. Fuel 116, 281–291.

Ma, X., Jiang, C., Xu, H., Shuai, S., Ding, H., 2013. Laminar burning characteristics of 2-methylfuran compared with 2, 5-dimethylfuran and isooctane. Energy & fuels 27, 6212–6221.

Ma, X., Xu, H., Jiang, C., Shuai, S., 2014b. Ultra-high speed imaging and OH-LIF study of DMF and MF combustion in a DISI optical engine. Appl. Energy 122, 247–260.

Mhadmhan, S., Franco, A., Pineda, A., Reubroycharoen, P., Luque, R., 2019. Continuous Flow Selective Hydrogenation of 5-Hydroxymethylfurfural to 2, 5-Dimethylfuran Using Highly Active and Stable Cu–Pd/Reduced Graphene Oxide. ACS Sustain. Chem. Eng. 7, 14210–14216.

Minh, T., Anh, T., 2018. Influences of heating temperatures on physical properties, spray characteristics of bio-oils and fuel supply system of a conventional diesel engine. Int. J.

Adv. Sci. Eng. Inf. Technol. https://doi.org/10.18517/ijaseit.8.5.5487

Murugesan, P., Hoang, A.T., Perumal Venkatesan, E., Santosh Kumar, D., Balasubramanian, D., Le, A.T., Pham, V.V., 2021. Role of hydrogen in improving performance and emission characteristics of homogeneous charge compression ignition engine fueled with graphite oxide nanoparticle-added microalgae biodiesel/diesel blends. Int. J. Hydrogen Energy. https://doi.org/https://doi.org/10.1016/j.ijhydene.2021.08.107

Naqash, M.T., Aburamadan, M.H., Harireche, O., AlKassem, A., Farooq, Q.U., 2021. The Potential of Wind Energy and Design Implications on Wind Farms in Saudi Arabia. Int. J. Renew. Energy Dev. 10, 839–856.

Nayak, S.K., Behera, G.R., Mishra, P.C., Kumar, A., 2017. Functional characteristics of jatropha biodiesel as a promising feedstock for engine application. Energy Sources, Part A Recover. Util. Environ. Eff. 39, 299–305. https://doi.org/10.1080/15567036.2015.1120826

Nayak, S.K., Huynh, T.T., Ölçer, A., Le, A.T., 2020. A remarkable review of the effect of lockdowns during COVID-19 pandemic on global PM emissions. Energy Sources, Part A Recover. Util. Environ. Eff. 1–16. https://doi.org/10.1080/15567036.2020.1853854

Nayak, S.K., Mishra, P.C., 2017. Analysis of a diesel engine fuelled with jojoba blend and coir pith producer gas. Int. J. Automot. Mech. Eng. 14, 4675–4689.

Nayak, S.K., Mishra, P.C., 2016. Emission from utilization of producer gas and mixes of jatropha biodiesel. Energy Sources, Part A Recover. Util. Environ. Eff. 38, 1993–2000. https://doi.org/10.1080/15567036.2014.987857

Nikkhah, A., Bagheri, I., Psomopoulos, C., Payman, S.H., Zareiforoush, H., El Haj Assad, M., Bakhshipour, A., Ghnimi, S., 2019. Sustainable second-generation biofuel production potential in a developing country case study. Energy Sources, Part A Recover. Util. Environ. Eff. 1–14.

Nishimura, S., Ikeda, N., Ebitani, K., 2014. Selective hydrogenation of biomass-derived 5-hydroxymethylfurfural (HMF) to 2, 5-dimethylfuran (DMF) under atmospheric hydrogen pressure over carbon supported PdAu bimetallic catalyst. Catal. Today 232, 89–98.

Noor, M.M., Pham, X.D., Tuan, H.A., 2018. Comparative Analysis on Performance and Emission Characteristic of Diesel Engine Fueled with Heated Coconut Oil and Diesel Fuel. Int. J. Automot. Mech. Eng. 15, 5110–5125. https://doi.org/10.15282/ijame.15.1.2018.16.0395

Norhafana, M., Noor, M.M., Sharif, P.M., Hagos, F.Y., Hairuddin, A.A., Kadirgama, K., Ramasamy, D., Rahman, M.M., Alenezi, R., Hoang, A.T., 2018. A review of the performance and emissions of nano additives in diesel fuelled compression ignition-engines, in: IOP Conference Series: Materials Science and Engineering. IOP Publishing, p. 12035.

Ohyagi, S., Harigaya, Y., Kakizaki, K., Toda, F., 2010. Estimation of Flame Propagation in Spark-Ignition Engine by Using Turbulent Burning Model.

Ölçer, A.I., Nguyen, X.P., Huynh, T.T., 2021. Record decline in global CO2 emissions prompted by COVID-19 pandemic and its implications on future climate change policies. Energy Sources, Part A Recover. Util. Environ. Eff. 1–4. https://doi.org/10.1080/15567036.2021.1879969

Ölçer, A.I., Nižetić, S., 2021. Prospective review on the application of biofuel 2, 5-dimethylfuran to diesel engine. J. Energy Inst. 94, 360–386. https://doi.org/10.1016/j.joei.2020.10.004

Ong, H.C., Nižetić, S., Mofijur, M., Ahmed, S.F., Ashok, B., Bui, V.T.V., Chau, M.Q., 2021a. Insight into the recent advances of microwave pretreatment technologies for the conversion of lignocellulosic biomass into sustainable biofuel. Chemosphere.

Ong, H.C., Nizetic, S., Ölçer, A.I., 2021b. Synthesis pathway and

combustion mechanism of a sustainable biofuel 2,5-Dimethylfuran: Progress and prospective. Fuel 286, 119337. https://doi.org/10.1016/j.fuel.2020.119337

Ong, V.Z., Wu, T.Y., 2020. An application of ultrasonication in lignocellulosic biomass valorisation into bio-energy and bio-based products. Renew. Sustain. Energy Rev. 132, 109924.

Onlamnao, K., Phromphithak, S., Tippayawong, N., 2020. Generating Organic Liquid Products from Catalytic Cracking of Used Cooking Oil over Mechanically Mixed Catalysts. Int. J. Renew. Energy Dev. 9.

Pandey, A., Huang, Z., Luque, R., Ng, Kim Hoong Papadopoulos, A., Chen, W.-H., Rajamohan, S., Hadiyanto, H., Pham, V., Nguyen, X., Hoang, A., 2022. Catalyst-based synthesis of 2,5-dimethylfuran from carbohydrates as sustainable biofuel production route. ACS Sustain. Chem. Eng.

Peña, G.D.J.G., Hammid, Y.A., Raj, A., Stephen, S., Anjana, T., Balasubramanian, V., 2018. On the characteristics and reactivity of soot particles from ethanol-gasoline and 2, 5-dimethylfuran-gasoline blends. Fuel 222, 42–55.

Pham, M.T., Le, T.H., Hadiyanto, H., Pham, V.V., Hoang, A.T., 2021. Influence of various basin types on performance of passive solar still: A review. Int. J. Renew. Energy Dev. https://doi.org/10.14710/IJRED.2021.38394

Pham, V.V., 2019. Technological perspective for reducing emissions from marine engines. Int. J. Adv. Sci. Eng. Inf. Technol. 9. https://doi.org/10.18517/ijaseit.9.6.10429

Pham, V.V., Hoang, A.T., 2019. A study of emission characteristic, deposits, and lubrication oil degradation of a diesel engine running on preheated vegetable oil and diesel oil. Energy Sources, Part A Recover. Util. Environ. Eff. 41, 611–625. https://doi.org/10.1080/15567036.2018.1520344

Pradhan, S., Ghose, D., Shabbiruddin., 2020. Present and future impact of COVID-19 in the renewable energy sector: A case study on India. Energy Sources, Part A Recover. Util. Environ. Eff. 1–11.

Praveena, V., Martin, L.J., Varuvel, E.G., 2021. Experimental evaluation of a compression ignition engine enacted with biofuel from beverage industry waste and higher grades of alcohol. Energy Sources Part A Recover. Util. Environ. Eff.

Przydacz, M., Jędrzejczyk, M., Rogowski, J., Szynkowska-Jóźwik, M., Ruppert, A.M., 2020. Highly Efficient Production of DMF from Biomass-Derived HMF on Recyclable Ni-Fe/TiO2 Catalysts. Energies 13, 4660.

Ramamoorthy, N.K., Nagarajan, R., Ravi, S., Sahadevan, R., 2020. An innovative plasma pre-treatment process for lignocellulosic bio-ethanol production. Energy Sources, Part A Recover. Util. Environ. Eff. 1–15.

Reddy, K.H., Nanthagopal, K., 2021. Investigations on compression ignition engine durability through long-term endurance study using low viscous biofuel blends. Clean Technol. Environ. Policy 23, 2413–2428.

Román-Leshkov, Y., Barrett, C.J., Liu, Z.Y., Dumesic, J.A., 2007. Production of dimethylfuran for liquid fuels from biomass-derived carbohydrates. Nature. https://doi.org/10.1038/nature05923

Roy, S., Zare, S., Askari, O., 2019. Understanding the effect of oxygenated additives on combustion characteristics of gasoline. J. Energy Resour. Technol. 141.

Sahu, A., Wang, C., Jiang, C., Xu, H., Ma, X., Xu, C., Bao, X., 2019. Effect of CO2 and N2 dilution on laminar premixed MTHF/air flames: Experiments and kinetic studies. Fuel 255, 115659.

Sahu, A.B., Markendaya, S., Badhuk, P., Ravikrishna, R. V, 2020. Experiments and Kinetic Modelling of Diffusion Flame Extinction of 2-Methylfuran, 2, 5-Dimethylfuran and Binary Mixtures with Isooctane. Energy & Fuels.

Sandro, N., Viet, P. van, 2020. A state-of-the-art review on emission characteristics of SI and CI engines fueled with 2,5-dimethylfuran biofuel. Environ. Sci. Pollut. Res. https://doi.org/10.1007/s11356-020-11629-8

Sauer, C., Lorén, A., Schaefer, A., Carlsson, P.-A., 2021.

Valorisation of 2, 5-dimethylfuran over zeolite catalysts studied by on-line FTIR-MS gas phase analysis. Catal. Sci. Technol.

Simsek, S., Uslu, S., Sahin, M., Arlı, F., Bilgic, G., 2021. Impact of a novel fuel additive containing boron and hydrogen on diesel engine performance and emissions. Energy Sources, Part A Recover. Util. Environ. Eff. 1–15.

Somers, K.P., Simmie, J.M., Gillespie, F., Conroy, C., Black, G., Metcalfe, W.K., Battin-Leclerc, F., Dirrenberger, P., Herbinet, O., Glaude, P.-A., 2013. A comprehensive experimental and detailed chemical kinetic modelling study of 2, 5-dimethylfuran pyrolysis and oxidation. Combust. Flame 160, 2291–2318.

Syukri, S., Ferdian, F., Rilda, Y., Putri, Y.E., Efdi, M., Septiani, U., 2021. Synthesis of Graphene Oxide Enriched Natural Kaolinite Clay and Its Application For Biodiesel Production. Int. J. Renew. Energy Dev. 10.

Tabatabaei, M., Aghbashlo, M., 2020. A review of the effect of biodiesel on the corrosion behavior of metals/alloys in diesel engines. Energy Sources, Part A Recover. Util. Environ. Eff. https://doi.org/https://doi.org/10.1080/15567036.2019.1623346

Tabatabaei, M., Aghbashlo, M., Carlucci, A.P., Ölçer, A.I., Le, A.T., Ghassemi, A., 2020. Rice bran oil-based biodiesel as a promising renewable fuel alternative to petrodiesel: A review. Renew. Sustain. Energy Rev. 135, 110204. https://doi.org/10.1016/j.rser.2020.110204

Tajuelo, M., Rodríguez, D., Rodríguez, A., Escalona, A., Viteri, G., Aranda, A., Diaz-de-Mera, Y., 2021. Secondary organic aerosol formation from the ozonolysis and oh-photooxidation of 2, 5-dimethylfuran. Atmos. Environ. 245, 118041.

Tang, C., Zhang, Y., Huang, Z., 2014. Progress in combustion investigations of hydrogen enriched hydrocarbons. Renew. Sustain. Energy Rev. 30, 195–216.

Teraji, A., Tsuda, T., Noda, T., Kubo, M., Itoh, T., 2005. Development of a novel flame propagation model (UCFM: universal coherent flamelet model) for SI engines and its application to knocking prediction. SAE Technical Paper.

Tham, B.C., Vang, L. Van, Viet, P. Van, 2019. An investigation of deposit formation in the injector, spray characteristics, and performance of a diesel engine fueled with preheated vegetable oil and diesel fuel. Energy Sources, Part A Recover. Util. Environ. Eff. 41, 2882–2894. https://doi.org/10.1080/15567036.2019.1582731

Thomas, S., Sandro Nižetić, Olcer, A.I., Ong, H.C., Chen, W.-H., Chong, C.T., Bandh, S.A., Nguyen, X.P., 2021. Impacts of COVID-19 pandemic on the global energy system and the shift progress to renewable energy: Opportunities, challenges, and policy implications. Energy Policy 154, 112322. https://doi.org/10.1016/j.enpol.2021.112322

Thu, N., Anh, H., 2017. Emission characteristics of a diesel engine fuelled with preheated vegetable oil and biodiesel. Philipp. J. Sci 146, 475–482.

Tian, G., Daniel, R., Li, H., Xu, H., Shuai, S., Richards, P., 2010. Laminar burning velocities of 2,5-dimethylfuran compared with ethanol and gasoline. Energy and Fuels. https://doi.org/10.1021/ef100452c

Tian, Z., Li, J., Yan, Y., 2019. A reduced mechanism for 2, 5-dimetylfuran with assembled mechanism reduction methods. Fuel 250, 52–64.

Togbé, C., Tran, L.-S., Liu, D., Felsmann, D., Oßwald, P., Glaude, P.-A., Sirjean, B., Fournet, R., Battin-Leclerc, F., Kohse-Höinghaus, K., 2014. Combustion chemistry and flame structure of furan group biofuels using molecular-beam mass spectrometry and gas chromatography–Part III: 2, 5-Dimethylfuran. Combust. Flame 161, 780–797.

Tran, D.Q., Tran, T.T., Le, A.T., 2020. Performance and combustion characteristics of a retrofitted CNG engine under various piston-top shapes and compression ratios. Energy Sources, Part A Recover. Util. Environ. Eff. 1–17. https://doi.org/10.1080/15567036.2020.1804016

Tran, Q.V., Nguyen, D.C., Hadiyanto, H., Wattanavichien, K., Pham, V.V., 2021. A review on the performance, combustion, and emission characteristics of spark-ignition engine fueled with 2, 5-Dimethylfuran compared to ethanol and gasoline. J. Energy Resour. Technol. 143, 40801.

Tse, S.D., Zhu, D.L., Law, C.K., 2000. Morphology and burning rates of expanding spherical flames in H2/O2/inert mixtures up to 60 atmospheres. Proc. Combust. Inst. 28, 1793–1800.

Tuan Anh, H., 2020. Applicability of fuel injection techniques for modern diesel engines, in: AIP Conference Proceedings. p. 020018. https://doi.org/10.1063/5.0000133

Van Pham, V., Anh Hoang, T., 2020. A study on a solution to reduce emissions by using hydrogen as an alternative fuel for a diesel engine integrated exhaust gas recirculation. Int. Conf. Emerg. Appl. Mater. Sci. Technol. ICEAMST 2020. https://doi.org/10.1063/5.0007492

Vieira, S., Barros, M.V., Sydney, A.C.N., Piekarski, C.M., de Francisco, A.C., de Souza Vandenberghe, L.P., Sydney, E.B., 2020. Sustainability of sugarcane lignocellulosic biomass pretreatment for the production of bioethanol. Bioresour. Technol. 299, 122635.

Viet Pham, V., Tuan Hoang, A., 2021. 2-Methylfuran (MF) as a potential biofuel: A thorough review on the production pathway from biomass, combustion progress, and application in engines. Renew. Sustain. Energy Rev. 148, 111265. https://doi.org/10.1016/j.rser.2021.111265

Vinayagam, N.K., Solomon, J.M., Subramaniam, M., Balasubramanian, D., EL-Seesy, A.I., Nguyen, X.P., 2021. Smart control strategy for effective hydrocarbon and carbon monoxide emission reduction on a conventional diesel engine using the pooled impact of pre-and post-combustion techniques. J. Clean. Prod. 306, 127310. https://doi.org/10.1016/j.jclepro.2021.127310

Vinh, Q.T., Duong, X.P., Anh, T.H., 2018. Performance and emission characteristics of popular 4-stroke motorcycle engine in vietnam fuelled with biogasoline compared with fossil gasoline. Int. J. Mech. Mechatronics Eng 18, 97–103.

Vo, A.V., Bui, V.G., Tran, V.N., Bui, T.M.T., 2020. A simulation study on a port-injection SI engine fueled with hydroxy-enriched biogas. Energy Sources, Part A Recover. Util. Environ. Eff. https://doi.org/10.1080/15567036.2020.1804487

vom Lehn, F., Cai, L., Cáceres, B.C., Pitsch, H., 2021. Exploring the fuel structure dependence of laminar burning velocity: A machine learning based group contribution approach. Combust. Flame 232, 111525.

Wahyono, Y., Hadiyanto, H., Budihardjo, M.A., Adiansyah, J.S., 2020. Assessing the environmental performance of palm oil biodiesel production in Indonesia: A life cycle Assessment approach. Energies 13, 3248.

Wang, S., Yao, L., 2020. Effect of Engine Speeds and Dimethyl Ether on Methyl Decanoate HCCI Combustion and Emission Characteristics Based on Low-Speed Two-Stroke Diesel Engine. Polish Marit. Res. 27, 85–95. https://doi.org/10.2478/pomr-2020-0030

Wang, X., Liang, X., Li, J., Li, Q., 2019. Catalytic hydrogenolysis of biomass-derived 5-hydroxymethylfurfural to biofuel 2, 5-dimethylfuran. Appl. Catal. A Gen.

Weerasinghe, W.M.L.I., Madusanka, D.A.T., Manage, P.M., 2021. Isolation and Identification of Cellulase Producing and Sugar Fermenting Bacteria for Second-Generation Bioethanol Production. Int. J. Renew. Energy Dev. 10, 699–711.

Wei, M., Li, S., Liu, J., Guo, G., Sun, Z., Xiao, H., 2017. Effects of injection timing on combustion and emissions in a diesel engine fueled with 2,5-dimethylfuran-diesel blends. Fuel. https://doi.org/10.1016/j.fuel.2016.11.084

Williams, F.A., 2018. Combustion theory. CRC Press.

Wirawan, I.K.G., Soenoko, R., Wahyudi, S., 2014. Premixed Combustion of Kapok (ceiba pentandra) seed oil on Perforated Burner. Int. J. Renew. Energy Dev. 3, 91.

Wu, F., Jomaas, G., Law, C.K., 2013. An experimental

investigation on self-acceleration of cellular spherical flames. Proc. Combust. Inst. 34, 937–945.

Wu, X., Huang, Z., Jin, C., Wang, X., Wei, L., 2010. Laminar burning velocities and Markstein lengths of 2, 5-dimethylfuran-air premixed flames at elevated temperatures. Combust. Sci. Technol. 183, 220–237.

Wu, X., Huang, Z., Jin, C., Wang, X., Zheng, B., Zhang, Y., Wei, L., 2009. Measurements of laminar burning velocities and Markstein lengths of 2, 5-dimethylfuran− air− diluent premixed flames. Energy & fuels 23, 4355–4362.

Wu, X., Huang, Z., Wang, X., Jin, C., Tang, C., Wei, L., Law, C.K., 2011. Laminar burning velocities and flame instabilities of 2, 5-dimethylfuran–air mixtures at elevated pressures. Combust. Flame 158, 539–546.

Wu, X., Li, Q., Fu, J., Tang, C., Huang, Z., Daniel, R., Tian, G., Xu, H., 2012. Laminar burning characteristics of 2, 5-dimethylfuran and iso-octane blend at elevated temperatures and pressures. Fuel 95, 234–240.

Xie, Y., Li, Q., 2019. Effect of the initial pressures on evolution of intrinsically unstable hydrogen/air premixed flame fronts. Int. J. Hydrogen Energy 44, 17030–17040.

Xu, N., Gong, J., Huang, Z., 2016. Review on the production methods and fundamental combustion characteristics of furan derivatives. Renew. Sustain. Energy Rev. 54, 1189–1211.

Xuan, N., Van, P., Anh, H., 2021. Use of Biodiesel Fuels in Diesel Engines, in: Biodiesel Fuels. CRC Press, pp. 317–341.

Xuan, P., Viet, P., 2021. Integrating renewable sources into energy system for smart city as a sagacious strategy towards clean and sustainable process. J. Clean. Prod. 305, 127161. https://doi.org/10.1016/j.jclepro.2021.127161

Ya, Y., Nie, X., Han, W., Xiang, L., Gu, M., Chu, H., 2020. Effects of 2, 5–dimethylfuran/ethanol addition on soot formation in n-heptane/iso-octane/air coflow diffusion flames. Energy 210, 118661.

Yin, C., Yan, J., 2016. Oxy-fuel combustion of pulverized fuels: Combustion fundamentals and modeling. Appl. Energy 162, 742–762.

Zhang, J., Zhang, X., Yang, M., Singh, S., Cheng, G., 2020. Transforming lignocellulosic biomass into biofuels enabled by ionic liquid pretreatment. Bioresour. Technol. 124522.

Zhang, L., Yang, K., Zhao, R., Chen, M., Ying, Y., Liu, D., 2020. Nanostructure and reactivity of soot from biofuel 2, 5-dimethylfuran pyrolysis with CO 2 additions. Front. Energy 1–15.

Zhang, Q., Chen, G., Zheng, Z., Liu, H., Xu, J., Yao, M., 2013. Combustion and emissions of 2, 5-dimethylfuran addition on a diesel engine with low temperature combustion. Fuel 103, 730–735.

Zhang, Y.-R., Wang, B.-X., Qin, L., Li, Q., Fan, Y.-M., 2019. A non-noble bimetallic alloy in the highly selective electrochemical synthesis of the biofuel 2, 5-dimethylfuran from 5-hydroxymethylfurfural. Green Chem. 21, 1108–1113.

Zhu, C., Wang, H., Li, H., Cai, B., Lv, W., Cai, C., Wang, C., Yan, L., Liu, Q., Ma, L., 2019. Selective Hydrodeoxygenation of 5-Hydroxymethylfurfural to 2, 5-Dimethylfuran over Alloyed Cu− Ni Encapsulated in Biochar Catalysts. ACS Sustain. Chem. Eng. 7, 19556–19569.

Zu, Y., Yang, P., Wang, J., Liu, X., Ren, J., Lu, G., Wang, Y., 2014. Efficient production of the liquid fuel 2, 5-dimethylfuran from 5-hydroxymethylfurfural over Ru/Co3O4 catalyst. Appl. Catal. B Environ. 146, 244–248.

Zullaikha, S., Putra, A.K., Fachrudin, F.H., Naulina, R.Y., Utami, S., Herminanto, R.P., Ju, Y.H., 2021. Experimental Investigation and Optimization of Non-Catalytic In-Situ Biodiesel Production from Rice Bran Using with RSM Historical Data Design. Int. J. Renew. Energy Dev. 10, 804–810.

ZuoHua, H., Sandro, N., Ashok, P., Xuan Phuong, Nguyen Rafael, L., Ongi, H.C., Zafar, S., Tri Hieu, L., Van Viet, P., 2021. Characteristics of hydrogen production from steam gasification of plant-originated lignocellulosic biomass and its prospects in Vietnam. J. Hydrog. Energy 1–20.